Progress in Fractional Differentiation and Applications
An International Journal

http://dx.doi.org/10.18576/pfda/090401

Mathematical Epidemiology: A Review of the Singular and Non-Singular Kernels and their Applications

Kottakkaran Sooppy Nisar [1,*], *Muhammad Farman*[2,3], *Mahmoud Abdel-Aty*[4,5], *Jinde Cao*[6,7]

[1] Department of Mathematics, College of Science and Humanities in Alkharj, Prince Sattam bin Abdulaziz University, Alkharj, 11942, Saudi Arabia
[2] Institute of Mathematics, Khwaja Fareed University of Engineering and Information Technology, Rahim Yar Khan, Pakistan
[3] Department of Computer Science and Mathematics, Lebanese American University, Beirut, Lebanon
[4] Deanship of Graduate Studies and Research, Ahlia University, Manama, Kingdom of Bahrain
[5] Mathematics Department, Sohag University, Egypt
[6] School of Mathematics, Southeast University, Nanjing 210096, China.
[7] Yonsei Frontier Lab, Yonsei University, Seoul 03722, South Korea

Received: 7 Apr. 2023, Revised: 24 Jun. 2023, Accepted: 26 Jun. 2023
Published online: 1 Oct. 2023

Abstract: Both mathematics and science are important for one another and have a close relationship. It is impossible to dispute the significance of mathematics in a number of scientific disciplines, including electrical engineering, physics, biology, and medicine. Due to a number of applications of mathematical biology in the twenty-first century, researchers have taken a special interest in this field. Due to the complexity of the underlying connections, both deterministic and stochastic epidemiological models are founded on an inadequate understanding of the infectious network. Over the past several years, the use of different fractional operators to model the problem has grown, and it is now a common way to study how epidemics spread. New fractional operators, the infectious disease model has been studied in this paper. By using different numerical techniques and the time fractional parameters, the mechanical characteristics of the fractional order model are identified. The uniqueness and existence have been established. The model's local and global stability analysis has been found. In order to justify the theoretical results, numerical simulations are carried out for the presented method in the range of fractional order to show the implications of fractional and fractal orders. We applied very effective numerical technique to obtain the solutions of the model and simulations. Also, we present conditions of existence for a solution to the purposed epidemic model and to calculate the reproduction number in certain state conditions of the analyzed dynamic system. Infectious disease fractional order model is offered for analysis with simulations in order to determine the possible efficacy of disease transmission in the Community. The Fractal fractional operator is employed to study the dynamical transmission of diseases effect on society which is helpful for analysis, decision making, and disease control. Are treated with the Banach contraction principle. Microorganisms, interactions between individuals or groups, and environmental, social, economic, and demographic factors on a broader scale are all examples. Finally, numerical simulations that demonstrate the impact of fractional parameters on our found solutions are built to study the impact of the system parameter on the disease's spread. In conclusion, fractional operators in mathematical models can help decision-makers make better choices regarding the course of action to take in an epidemic situation. Further, we suggested some future work directions with the help of the new hybrid fractional operator. Fractional Calculus is a prominent topic for research within the discipline of Applied Mathematics due to its usefulness in solving problems in many different branches of science, engineering, and medicine. Recent researchers have identified the importance of mathematical tools in various disease models as being very useful to study the dynamics with the help of fractional and integer calculus modeling.

Keywords: Epidemic model, fractional derivative, integral inequality, singular, non-singular, constant proportional, kernels.

1 Introduction

A mathematical model is a made-up micro world where objects act in accordance with well-defined rules. In order to express these principles of behavior in a clear and succinct manner, mathematics gives us a language, which forces and

* Corresponding author e-mail: n.sooppy@psau.edu.sa

aids us in stating our assumptions. Once a mathematical model has been created, mathematical analysis often accompanied with computer simulations helps us explore the model's overall behavior and uncover the implications of our assumptions. when a result, within the framework of the model, we are able to anticipate the future of our fictional world and investigate how these predictions vary when the laws regulating the entities the model describes change [1]. An ecologically imbalanced interaction between a microbial infectious agent and a host leads to infectious illnesses. As a result [2] provides information on the population's exposure and environmental impact. In this regard, it is crucial to comprehend how the aforementioned components interact in order to foster the creation of efficient management, health aid, and policy measures [3]. Because of biological evolution, as well as social and environmental changes brought on by industrialization and development, epidemiological scales of viral illnesses are uncertain. The modifications are unavoidable and can't be stopped [4,5,6]. Frequent diseases among humans such as tuberculosis (TB), polio, smallpox, and diphtheria significantly exacerbated death and disability prior to the development of vaccinations [7]. There nonetheless exists an immense burden of infectious illness on lower and middle-income economies, especially neglected tropical diseases, HIV infection, tuberculosis, and malaria exhibiting high mortality and morbidity rates. Contrary to periodic and endemic ailments, mortality from new and reappearing pathogens remains elevated [8]. Within the last seventy years, the analysis of infectious disease patterns has developed into a complex, interdisciplinary field that combines epidemiology, health care administration, social science, philosophy, mathematics, and biology to comprehend and forecast the progression of the disease [9,10]. Some application with fractional order model for natural and biological phenomena studied in [11,12,13] and some epidemic model with fractional such as Marburg virus [14], cancer [15].

Late in 2019, a new epidemiological disease was identified in Wuhan, a city in the Chinese province of Hubei. The new beta coronavirus, which has a serious impact on the human respiratory system, was identified by researchers as the infectious disease's root cause. Chinese authorities identified the virus as practical, capable of spreading disease, in the beginning of January 2020. The virus caused the problem [16]. When the disease dynamics of a novel infection are still unknown, mathematical modelling is used to estimate the number of patients in worst- and best-case scenarios [17,18]. For the purpose of better understanding the dynamics of the COVID-19 transmission model, numerous mathematical models have been created and to offer health authorities with additional information on how to restrict the disease's spread [19,20]. In an attempt to provide an adequate dynamical framework to investigate the evolution of pandemic propagation, a number of scholars have presented fractional-order dynamical models for analyzing viral transmission. Numbers were utilized to quantitatively depict the COVID-19 epidemic as isolated classes in fractional order [21]. They applied the modified predictor-corrector approach and the fourth-order Runge-Kutta (RK4) technique to recreate the proposed model. Q-homotopy examination, a rapid and effective quantitative technique, was utilized by Yadav et al. [22] to analyze the fractional order Covid-19 model. We applied the Liouville-Caputo approach to the fractional operator. A quantitative evaluation of the suggested model was done as well using the generalized Adams-Bashforth-Moulton methodology. Fractal fractional, Atangana-Baleanu, and Atangana-Toufik Farman et al. [23] created fractional derivatives for the COVID-19 model using Atangana-Baleanu senses. Understanding the COVID-19 outbreak is made easier by these cutting-edge methods. The generalized Mittag-Leffler law was used to solve the issue together with different fractional operators. A comprehensive examination of a four-compartment COVID-19 mathematical model was carried out in [24]. Fuzzy and random methods were used to handle the unique COVID-19 model, and the Adams-Bashforth method was used to find the numerical answers for the arbitrary model. In addition, they investigated the suggested model under ABC derivatives through numerical simulations adopting the fractional Adam Bashforth method. Antiviral HIV therapies have reduced AIDS fatalities globally, and organizations around the world are attempting to make preventative and curative therapies more widely available in underdeveloped nations. In the fractional order HIV/AIDS model, Khan et al. [25] investigated the Liouville-Caputo and Atangana-Baleanu-Caputo derivatives. The Laplace and Sumudu transforms were used to generate the specific iterative results. To research the impact of HIV viral screening on the transmission among those who aren't aware they are infected, [26] developed a model of the human immunodeficiency virus infection's fractional order spread. Using Caputo-Fabrizio and fractal fractional methods, a fractional-order model of HIV/AIDS including a section for antiretroviral treatments was investigated in [27]. The Sumudu transform was used to get the findings for the proposed concepts. Some application of modified Atangana-Baleanu [28], piecewise fractional analysis [29], intravenous drug model [30],piecewise constant for chemo-immunotherapy [31] and SEIQR model [32].

The Ebola virus causes ebola, a viral hemorrhaging illness that infects humans and primates as well. In sub-Saharan Africa's tropical regions, ebola outbreaks come and go. The World Health Organization reports that there were 24 Ebola outbreaks between 1976 and 2012, totaling 2,387 cases and 1,590 fatalities [33]. Ebola virus (Ebola) outbreaks destroyed large populations in Western Africa in 2014. This epidemic was the deadliest among Ebola threats since 1976, with more than 16,000 clinically confirmed cases and almost 70% death cases [34]. The epidemic is primarily occurring in a region with weak public health infrastructure [35]. There are four distinct Ebola virus species that can be found in west or

equatorial Africa. When the more virulent variants reach the human population, they spread mostly by contact with bodily fluids that are contaminated and can cause significant epidemics in places with inadequate resources. Extensive replication of the virus, decreased immunity, abnormal reactions to inflammation, considerable fluid and electrolyte expenses, and high mortality are characteristics of a disease caused by these viruses [36]. To model the transmission of this disease in the three nations afflicted by the 2014 outbreak Guinea, Liberia, and Sierra Leonea number of methods have been put forth. By including a second variable for the number of vaccines, [37] considers the optimum control problem of the Ebola epidemic with vaccination limitations and transmission in [38]. A key defense against Ebola virus outbreaks is the isolation method, which is used when there is no effective treatment or vaccine. A deterministic compartmental model for evaluating the effects of isolation to contain the Ebola virus was provided by researchers in [39]. The demographic effects, latent detectable and undetectable compartments, and separation of infectious persons were all considered in the model. To comprehend the spread of this epidemic disease, Farman et al. [40] provided a nonlinear time-fractional mathematical model of the Ebola Virus. Cancer is a complex illness characterized by multiple tempo-spatial alterations in cell physiology that eventually lead to malignant tumors. The disease's biological goal is abnormal cell proliferation (neoplasia). The primary cause of illness and mortality in most cancer patients is tumor cell invasion of surrounding tissues and distant organs. According to the research, around $25-30\%$ of all cancer-related fatalities are caused by cigarettes, $30-35\%$ by diet, $15-20\%$ by infections, and the remainder by other variables such as radiation, stress, physical activity, environmental contaminants, and so on [41,42]. Cancer incidence appears to be substantially lower in many developing countries, most likely due to increased death rates from infectious disease or injury. Cancer incidence is anticipated to rise by 100% to 180% over the next 15 years as life expectancy rises, the senior population grows, and childhood disease is successfully controlled [43]. Some application of mathematics for different types of cancer studied in [44,45].

Panda et al. [46,47] provide useful advice for figuring out whether the novel coronavirus model can be solved using fractional derivatives with fuzzy mappings. We looked into the fractional operators from the Caputo, Caputo-Fabrizio, and Atangana-Baleanu classes. Numerous mathematical concepts created by Atangana and Araz have recently been used to predict how infectious disease transmission will behave. Among these, the reproductive number idea has been used to analyze the stability of the spread in a number of published articles. A number of conditions were presented to indicate whether [48] would be stable or unstable. Atangana and Baleanu developed a fractional order derivative to answer numerous important problems in fractional calculus. Non-locality and non-singularity make up the core of their derivation. We accomplish a chaotic behaviour that the local derivative could not have generated [49].We explored some of the favourable properties of the new derivative and applied them to solve the fractional heat transfer model. It is suggested that new derivatives with nonlocal and nonsingular kernels be used in this work [50]. Atangana developed useful tools that could be used to apply the new derivative to the nonlinear Fisher's reaction-diffusion equation. We provided a solution to the altered equation using the concept of an iterative process. Using the notion of fixed points, [51] we proved the strategy's stability. On some information theory-based research projects, Atangana and Badr collaborated. We also discuss the existence of the connected solutions in terms of the fixed-point theorem. A full analysis of the singularity of the coupled solutions is also given. We create distinct coupled solutions for the modified system using an iterative procedure, and [52] In order to provide, on the one hand, the many definitions of fractional calculus for practical issues in [53], Atangana and Secer created this remark. In this study, it is suggested to approximate the numerically generated fractional derivative by Atangana and Nieto. Along with a number of numerical simulations for various orders of derivation, the updated equation can be solved. The African Humid Tropics (AHT) have been the attention of Tchoundjeu et al. [54] since 1987. Despite having access to abundant natural resources, the small-scale farmers in AHT are among the world's poorest. They have traditionally relied on subsistence agriculture and the extraction of forest products for their food and other necessities. Alternatives must now be explored as a result of rising land pressure and falling cash crop commodity prices after years of disastrous deforestation. According to a study by Tchientche et al. [55], promoting the consumption of local vegetables could assist develop countries reduce malnutrition and food insecurity. According to research by Aguilar and Atangana, the exponential decay law or the Mittag-Leffler law can explain some physical occurrences in nature but the power law cannot. We propose a power-law exponential Mittag-Leffler kernel in this paper with three fractional orders. Numerous beneficial traits are acquired. For the three instances mentioned in [56], numerical solutions were found. The exponential kernel, Caputo-Fabrizio derivative, and Hilfer fractional derivative are employed in a novel fractional model for the human liver [57,58].

The system behaves consistently even when the fractal order π fluctuates and the fractional order value $\nu = 0.5$. Considering the intricacy and nonlinearity of the problem, the Adams-Bashforth method was used in [59]. Describes a numerical method [60] for predicting the parameters of fractional-order corona virus systems using a modified hybrid method and fractional recovery SIR models [61] under appropriate restrictions. The Adams technique was statistically simulated by the researchers using data from the Cape Verdean islands dengue fever outbreak in 2009. Fractional derivatives [62] in dengue outbreaks were used in this simulation. It is evident that both fractional models provide results

that are almost equal up until the highest level of the affected population, but the system with the changed parameters better replicates the epidemic's latter stages [63]. Time-fractional PDEs were analyzed using convergent series with calculable components, which is a recently created analytical technique known as the $q-$ Homotopy analysis approach [64]. Fixed point theory was implemented to examine the existence and uniqueness of the solution to the fractional-order epidemic model of childhood diseases [65]. [66] looked explored the conditions for fractional reverse and fractional Hopf bifurcation. They examined equilibrium stability and the stability of the Hopf bifurcation with regard to the illness control parameter, the dread intensity, and fractional order [67]. The integer order version of the original SIR epidemic model is stable. When periodic and noisy forces are applied to the system, the behavior of the system changes. The system's numerous dynamical tendencies are illustrated by its level of fractional derivative order, seasonality, and noise, together with different system attributes [68]. We can examine and predict the entire tumor-formation process using this model [69]. According to A. Atangana et al. [70]'s study, the A-B fractional derivative, which is based on the generalized Mittag-Leffler function, enhances the chaotic behaviors of the membrane potential's spiking-bursting conduct in photographs. Particularly obvious is the transition from the extended exponential to the generalized M-L function-induced trend. This should be contrasted with the outcomes attained when the model was constructed using a common differential operator. The fractional order recovery model is studied by C. N. Angstmann et al. [71], who mention model reduction to the Kermack-McKendrick age-structured SIR model and the Hethcote-Tudor integral equation SIR model. By transforming the logic from a continuous-time stochastic process to a discrete-time one, the model equations can be solved analytically. Additional methods for predicting the progression of the disease and, in some cases, influencing how long it requires to reach stable states have been made available through fractional derivatives. Our upcoming study will explore regulating the vaccination term u [72] in order to obtain a more optimum strategy with additional fractional derivatives with a non-singular kernel. Using GMMP and MH-NMSS-PSO, this work by T. Li et al. [73] calculated fractional-order dengue fever system parameters. Because of additional fractional orders and parameters, the numerical findings closely matched the data. In order to take advantage of the fractional order derivative of Atanagana-Baleanu, the findings are thus obtained and shown in [74] utilizing the recently proposed method, which is effectively applied to a variety of real-world applications. The value of $\alpha = 1, 0.95, 0.9, 0.85$ and the graphical results for the fractional dengue model were both attained. Contrary to integer order derivative, the graphical results demonstrate that useful information may be obtained at each time level and derivative. In the examination of dengue data, the vector host model performs better than the SIR model. For the purpose of reducing the number of infected and vulnerable populations and increasing the number of recovered groups, the fractional optimal control challenge for this fractional dynamic system is investigated. Additionally, a plan for an analytical approach to solving the issue is offered. In addition to modelling epidemics, the proposed method might also be utilized to model wireless sensor network switching stability and data packet delay dynamics [75]. Due to the difficulty of dealing with stochastic and random factors and the potential cost implications of dealing with uncertainty, fuzzy ideas may be the best option for simulating these systems in reality [76].

Scientists and scholars are paying increasing attention to a mathematical model of infectious disease that uses non-integer order. Undoubtedly, traditional epidemiological models can only be specified through a definite order, in contrast to fractional order derivative models, which do not have a fixed order. The non-fixed order of the fractional derivative improves its modelling skills. As new fractional operator ideas created to address the shortcomings of prior fractional order derivatives, the exponential decay, power law kernel, Mittag-Leffler kernel, and certain hybrid operators are employed for the epidemic model. With these fresh operators, modelling problems that occur in technology and research has been effective. A relatively new operator in fractional calculus is the fractal-fractional operator. Fractional order modelling, which is an extension of the integer-order derivative, is a helpful technique for studying the nature of diseases. In addition, a new parameter introduced by the fractional order system can improve mathematical simulations. After making an overview, we discuss a number of problems with these representations, look at some interesting methods for giving them generic systems, and suggest a different strategy: fractional calculus. Its main advantages include reality capture, memory-related capture, multistage construction, and improved data fitting. Fractional epidemic models provide a potent tool for doing so compared to integer-order models, which either ignore or make it impossible to account for the memory and heredity aspects of the systems. When it comes to data fitting, the fractional variant provides one more degree of independence than the integer model. Finally, we suggest that the concerned parties might gain from the development of numerical techniques that allow mathematical models to be fitted to actual data.

2 Definitions Related to Fractional Calculus

In any event, any model based on classical derivatives, we have some constraints due to the order of differential equations being considered. To get over these limitations, several authors have turned to fractional calculus, a relatively new branch of mathematics. The differential operators employed in fractional calculus are fractional order or non-integer, which have memory features and can be utilized to demonstrate a variety of natural occurrences, facts and

natural truths with anomalous behaviour and nonlocal dynamics. Researchers are very interested in fractional calculus [77]. In [78,79] researchers used various mathematical strategies to extend classical calculus to the fractional order using fractional order modelling. The residual power series method, spectral methods, method of collocation and Fourier transform method, as well as other new computer approaches, have recently been employed to manage classical and fractional order differential equations and associated systems [80,81]. Since fractional-order models have been used to anticipate dynamical real-world procedures, mathematical modelling of dynamical real-world processes or phenomena is quite good. The operators described have emerged in a variety of domains, including chemistry, physics and engineering.Researchers' interest in the fields of mathematics [82], engineering, biology [83] and fluid mechanics [84]. Recently, several fractional order mathematical models have been investigated by researchers for diseases like Hepatitis B [85], HIV/AIDS with new fractional techniques in [86], Covid-19 [23], TB [87] etc.

This section will describe the basic notions, and concepts of fractional operators that will be helpful, as well as the models, and methods, used in further chapters.

2.1 Riemann-Liouville

Some of the original most commonly used structures of fractional operators were evolved by Riemann and Liouville.

Definition 1.*[88] Consider a function $Z(t)$ where $Z(t) \in H^1[0,T],\ T > 0$. Let $0 < \alpha < 1$, then the Riemann-Liouville fractional integral of $Z(t)$ is defined as*

$$^{RL}I_{0,t}^{\alpha}(Z(t)) = \frac{1}{\Gamma(\alpha)} \int_0^t (t-\tau)^{\alpha-1}[Z(\tau)]d\tau. \tag{1}$$

2.2 Caputo Fractional Derivative

To overcome the hassles related to physical problems in Riemann Liouville, Caputo introduced new fractal operator. In real-world complications, it permits to use of both conditions initial and boundary and is very effective for modeling.

Definition 2.*[89] A Caputo derivative of fractional order $\rho \in [0,1]$, for the function $Z(t)$ can be defined as*

$$^{C}D_t^{\alpha}(Z(t)) = \frac{1}{\Gamma(n-\alpha)} \int_0^t \frac{Z^n(\tau)}{(t-\tau)^{\alpha-n+1}}]d\tau, \quad n = [\alpha]+1. \tag{2}$$

Definition 3.*[89] The corresponding integral operator of fractional order $\alpha \in [0,1]$ is defined:*

$$^{C}I_t^{\alpha}(Z(t)) = \frac{1}{\Gamma(\alpha)} \int_0^t (t-\tau)^{\alpha-1} Z(\tau)d\tau. \tag{3}$$

2.3 Caputo-Fabrizio Fractional Derivative

Definition 4.*[88] Consider a function, $Z(t)$ and $Z(t) \in H^1[0,\mathbb{T}],\ \mathbb{T} > 0$. Let $\alpha > 0$ and $n-1 < \alpha < n,\ n \in \mathbb{N}$, then the Caputo-Fabrizio derivative is defined as:*

$$^{CF}D_{0,t}^{\alpha}(Z(t)) = \frac{M(\alpha)}{1-\alpha} \int_0^t \alpha^{'}(\tau)\exp[\frac{\alpha(\tau-t)}{1-\alpha}]d\tau, \tag{4}$$

where $M(0) = 0 = M(1)$.

Definition 5.*[88] The Caputo-Fabrizio integral is defined as*

$$^{CF}I_{0,t}^{\alpha}(Z(t)) = \frac{2(1-\alpha)}{(2-\alpha)M(\alpha)}\rho(t) + \frac{2\alpha}{(2-\alpha)M(\alpha)} \int_0^t Z(\tau)d\tau. \tag{5}$$

2.4 Atangana-Baleanu-Caputo Fractional Derivative

Definition 6.*[50] Antagana-Baleanu-Caputo (ABC) can be defined as:*

$$ {}^{ABC}_{0}D_t^{\alpha}(Z(t)) = \frac{AB(\alpha)}{1-\alpha}\int_{\alpha}^{t}\frac{d}{d\tau}Z(\tau)E_{\alpha}\left(-\alpha\frac{(t-\tau)^{\alpha}}{1-\alpha}\right)d\tau \tag{6} $$

Where E_α is the Mittag-Leffler function and $AB(\alpha)$ is a normalization function.

*Remark.*For eq (6), a Laplace transformation is presented as:

$$ L[{}^{ABC}_{0}D_t^{\alpha}(Z(t))](S) = \frac{AB(\alpha)}{1-\alpha}\frac{S^{\alpha}L[Z(\tau)](S) - S^{\alpha-1}Z(0)}{S^{\alpha}+\frac{\alpha}{1-\alpha}}. \tag{7} $$

using ST for (6), we obtain

$$ ST[{}^{ABC}_{0}D_t^{\alpha}(Z(t))](S) = \frac{AB(\alpha)}{1-\alpha+\alpha S^{\alpha}}[STZ(t) - Z(0)]. \tag{8} $$

Definition 7.*Atangana-Baleanu fractional integral of order α of a function $Z(t)$ can be expressed as [90]*

$$ {}^{ABC}_{0}I_t^{\alpha}(Z(t)) = \frac{1-\alpha}{AB(\alpha)}Z(t) + \frac{\alpha}{AB(\alpha)\Gamma(\alpha)}\int_{\alpha}^{t}Z(\tau)(t-\tau)^{\alpha-1}d\tau. \tag{9} $$

2.5 Modified Atangana-Baleanu Derivative in Caputo sense

Definition 8.*[91] Let $Z \in L^1(0,T)$, the MABC derivative of order $0 < \alpha < 1$, is defined by*

$$ \begin{aligned} &{}^{MABC}D_0^{\alpha}Z(t) \\ &= \frac{AB(\alpha)}{1-\alpha}\left[Z(t) - E_{\alpha}(-\mu_{\alpha}t^{\alpha})Z(0) - \mu_{\alpha}\int_{0}^{t}(t-\tau)^{\alpha-1}E_{\alpha,\alpha}\left(-\mu_{\alpha}(t-\tau)^{\alpha}\right)Z(\tau)d\tau\right], \end{aligned} \tag{10} $$

where $\mu_\alpha = \frac{\alpha}{1-\alpha}$ and

$$ AB(\alpha) = 1-\alpha+\frac{\alpha}{\Gamma(\alpha)}. \tag{11} $$

The Laplace transform of MABC derivative is as follows:

$$ \mathscr{L}\left\{{}^{MABC}D_t^{\alpha}Z(t);s\right\} = \frac{AB(\alpha)}{(1-\alpha)}\frac{s^{\alpha}\mathscr{L}\{Z(t);s\} - s^{\alpha-1}Z(0)}{s^{\alpha}+\mu_{\alpha}}, \quad \left|\frac{\mu_{\alpha}}{s^{\alpha}}\right| < 1. \tag{12} $$

2.6 Fractal-Fractional Operators

Definition 9.*[92] Let $0 \le \alpha$, $\beta \le 1$ then $Z(t)$ in the Riemann-Liouville for fractal fractional operator for power law kernel is defined as :*

$$ {}^{FFP}D_{0,t}^{\alpha,\beta}(Z(t)) = \frac{1}{\Gamma(n-\alpha)}\frac{d}{dt^{\beta}}\int_{0}^{t}(t-\tau)^{n-\alpha-1}Z(\tau)d\tau \tag{13} $$

$$ \frac{d}{d\tau^{\beta}}Z(\tau) = lim_{t\to\tau}\frac{Z(t)-Z(\tau)}{t^{\beta}-\tau^{\beta}} \tag{14} $$

The associated integral is defined as:

$$ {}^{FFP}I_{0,t}^{\alpha,\beta}(Z(t)) = \frac{1}{\Gamma(\alpha)}\int_{0}^{t}(t-\tau)^{\alpha-1}\tau^{1-\beta}Z(\tau)d\tau \tag{15} $$

Definition 10.*[92] Let $0 \leq \alpha$, $\beta \leq 1$ then $Z(t)$ in the Riemann-Liouville for fractal fractional operator having exponentially decaying kernel is given as :*

$$^{FFE}D_{0,t}^{\alpha,\beta}(Z(t)) = \frac{M(\alpha)}{\Gamma(n-\alpha)}\frac{d}{dt^{\beta}}\int_0^t \exp[-\frac{\alpha}{1-\alpha}(t-\tau)^{n-\alpha-1}]Z(\tau)d\tau \tag{16}$$

where $\alpha > 0$, $\beta \leq n \in N$, and $M(0) = M(1) = 1$.
The associated integral is given by:

$$^{FFE}D_{0,t}^{\alpha,\beta}(Z(t)) = \frac{\beta(1-\alpha)t^{\beta-1}Z(t)}{M(\alpha)} + \frac{\alpha\beta}{M(\alpha)}\int_0^t \tau^{\alpha-1}Z(\tau)d\tau \tag{17}$$

Definition 11.*[92] Let $0 \leq \alpha$, $\beta \leq 1$ then $Z(t)$ in the Riemann-Liouville for fractal fractional operator with generalized Mittag-Leffler kernel (FFM) is defined as:*

$$^{FFM}D_{0,t}^{\alpha,\beta}(Z(t)) = \frac{AB(\alpha)}{1-\alpha}\frac{d}{dt^{\beta}}\int_0^t E_{\alpha}[-\frac{\alpha}{1-\alpha}(t-\tau)^{\alpha}]Z(\tau)d\tau \tag{18}$$

where $0 < \alpha, \beta \leq 1$ and $AB(\alpha) = 1-\alpha+\frac{\alpha}{\Gamma(\alpha)}$.
The related integral is given by:

$$^{FFM}D_{0,t}^{\alpha,\beta}(Z(t)) = \frac{\beta(1-\alpha)t^{\beta-1}Z(t)}{AB(\alpha)} + \frac{\alpha\beta}{AB(\alpha)}\int_0^t \tau^{\alpha-1}(t-\tau)Z(\tau)d\tau \tag{19}$$

2.7 Proportional and Hilfer Generalized Operators

Definition 12.*In [93] ,the general non-fractional differential operator, also familiar as Proportional or Conformable, was presented as;*

$$^{P}D_t^{\alpha}Z(t) = K_1(\alpha,t)Z(t) + K_0(\alpha,t)Z'(t) \tag{20}$$

$$\text{where} \qquad K_0(\alpha,t) = \alpha t^{1-\alpha} \ , \ K_1(\alpha,t) = (1-\alpha)t^{\alpha} \tag{21}$$

Moreover, K_0 and K_1 are functions of t and $\alpha \in [0,1]$, which satisfy the conditions given below $\forall t \in \mathbb{R}$

$$\lim_{\alpha\to 0^+} K_0(\alpha,t) = 0, \quad \lim_{\alpha\to 1^-} K_0(\alpha,t) = 1, \ K_0(\alpha,t) \neq 0, \quad \alpha \in (0,1] \tag{22}$$

$$\lim_{\alpha\to 0^+} K_1(\alpha,t) = 1, \quad \lim_{\alpha\to 1^-} K_1(\alpha,t) = 0, \ K_1(\alpha,t) \neq 0, \quad \alpha \in [0,1) \tag{23}$$

Moreover, a special case, can be compelling for us, where the functions K_0 and K_1 are constants with respect to t , depending on α only, known as Constant Proportional (CP) operator and is defined as follows;

$$^{CP}D_t^{\alpha}Z(t) = K_1(\alpha)Z(t) + K_0(\alpha)Z'(t) \tag{24}$$

Definition 13.*In [94] , a Hybrid Fractional Operator,known as Proportional-Caputo (PC),was developed by merging the Proportional Operator and Caputo Fractional Derivative;*

$$^{PC}_{0}D_t^{\alpha}Z(t) = \frac{1}{\Gamma(1-\alpha)}\int_0^t \Big(K_1(\alpha,\tau)Z(\tau) + K_0(\alpha,\tau)Z'(\tau)\Big)(t-\tau)^{-\alpha}d\tau \tag{25}$$

$$= {}^{RL}_{0}I_t^{1-\alpha}\Big[K_1(\alpha,t)Z(t) + K_0(\alpha,t)Z'(t)\Big] \tag{26}$$

Consider the case, when K_0 and K_1 are independent of t as in the $^{CP}D_{\alpha}$, known as Constant Proportional-Caputo (CPC)operator and is expressed as follows;

$$^{CPC}_{0}D_t^{\alpha}Z(t) = \frac{1}{\Gamma(1-\alpha)}\int_0^t \Big(K_1(\alpha)Z(\tau) + K_0(\alpha)Z'(\tau)\Big)(t-\tau)^{-\alpha}d\tau \tag{27}$$

$$= K_1(\alpha)\,{}^{RL}_{0}I_t^{1-\alpha}Z(t) + K_0(\alpha)\,{}^{C}_{0}D_t^{\alpha}Z(t) \tag{28}$$

Definition 14.*[95] If $\alpha \in (0,1]$ and $\gamma \in \mathbb{C}$, $Re(\gamma) > 0$.The fractional operator*

$$_{c}I_t^{\gamma,\alpha}Z(t) = \frac{1}{\alpha^{\gamma}\Gamma(\gamma)}\int_c^t e^{\frac{\alpha-1}{\alpha}(t-\tau)}(t-\tau)^{\gamma-1}Z(\tau)d\tau \tag{29}$$

is known as the left-sided generalized proportional integral of order γ of the function Z.

3 Contribution of Fractional on Epidemic Model

Colonialism, enslavement, and conflict contributed to the global spread of deadly diseases in premodern times. Over the past two decades, improvements in hygiene, healthcare accessibility, and medicine have reduced viral illnesses' mortality and morbidity. However, the burden of infectious diseases remains significant in low and lower middle-income countries, with HIV, tuberculosis, malaria, and neglected tropical diseases still being highly related to mortality and morbidity [96]. A mathematical model follows pre-established rules, allowing us to explain and examine assumptions' implications. Analysis and simulations help determine the model's behavior and consequences. Understanding pathophysiology and transmission of infectious diseases is crucial for prevention and control. Scientists create models to forecast disease spread and infection numbers using mathematical data and interactions between hosts, pathogens, or vectors [97]. Khan et al. developed a mathematical model for COVID-19 using the omicron variant, highlighting the impact of fear on people's actions and reducing new cases [98]. Zhang et al. developed a model for assessing diabetic patients' microvascular perfusion and early-stage artery damage [99]. Mathematical model for Ebola virus population dynamics, including bats, immune response, and vaccine [100]. Fractional calculus is a mathematical field that explores real and complex number powers of differentiation and integration operators. It is used in historical modeling and has properties beyond conventional derivatives. Fractional derivatives and integrals are not local attributes, making them useful in medical fields [101].

Farman and colleagues [102] suggested a LADM approach for fractional order model. According to Lyapunov's theory, Dhanalakshmi et al. [103] published a stability study of a fractional-order tumour system that correlates tumor-immune with treatment. The use of the reduced differential transform technique for two fractional-order cancer tumour models in the Caputo sense is discussed in [104]. To examine the consequences of heterogeneous vector biting exposure on the human population, researchers [105] developed and tested a fractional-order model for malaria disease transmission utilizing the Atangana-Baleanu derivative in Caputo sense. The nonlinear delayed Ross-Macdonald model for malaria transmission was generalized to a unique fractional-order model in [106], which improved the dynamics and added complexity. A stochastic model for co-infection with pneumonia and typhoid was published in [107] to examine the varied connections between the two diseases under the effect of preventative measures that consider environmental noise and piecewise fractional derivative operators, as well as some applications in [108]. A compartmental model for the transmission of dengue fever with nonlinear forces of infection via fractional derivative was created in citation 130. Researchers evaluated a dengue epidemic model with an Atangana-Baleanu fractional derivative using some well-known results from fixed point theory [109]. [110] makes an attempt to imitate the use of illegal drugs by combining the Mittag-Leffler kernel with the Atangana-Baleanu fractional derivative. In comparison to the deterministic heroin epidemic model the stochastic model is more accurate [111]. A heroin model is proposed with ABC derivative in [112], and some others operator used in [113, 114, 115]

Using a fractional derivative from Caputo and Fabrizo, researchers [116] have looked at a biological smoking model. A nonlinear fractional mathematical model for the smoking pandemic that takes into account two age groups is presented in [117]. Often emphasizes using the Caputo-Fabrizio differential operator [118] to analyze the dynamics of the fractional order stopping smoking model. Zeb [119] used fractional for smoking and some others include in [120, 121]. A fractional-order derivative [122] for a complex system of glucose-insulin regulation; [123] employed the Atangana-Baleanu derivative to analyze the fractional optimal control model for COVID-19 and diabetes co-dynamics. The study of a model for diabetes awareness that is created by a nonlinear interaction between the number of diabetes patients and the cumulative density of awareness-raising campaigns is illustrated by [124], which shows potential results. The novel fractional for glucose-insulin regulatory system on diabetes mellitus using the Atangana Baleanu-Caputo derivative along with stability results was explored by researchers [125]. A fractional-order mathematical model with three parts was created by [126] for communities of people with diabetes. The effectiveness of neural networks and fractional order calculus for system identification has been demonstrated. In their publication [127], they applied these approaches to build a fractional order neural network (FONN) for system identification. [128] investigated the stability studies for fractional-order Hopfield type neural networks. For neural networks with ring or hub architectures, the stability area of a steady state has been extensively characterised, and the critical fractional order values for which Hopf bifurcations may occur have been discovered [129]. An example of fractional-order neural networks with mixed delays that exhibit periodic oscillation caused by delays in [130]. In [131] demonstrated how fractional-order cellular neural networks may be optimized by using metaheuristics like DE and APSO.

[132] developed a fractional Zika virus model with a mutation that results in birth abnormalities in infected pregnant women and distributes the illness through society. A mathematical model for the Zika virus was provided and examined by [133], and the results were thoroughly examined. In [134] addressed the fractional mathematical model that represents the kinetics of the Zika virus's spread, one of the VBDs. In [135] suggested employing delay differential equations of fractional order to create an epidemiological model for the Zika virus. A fractional-order derivative-based model for the growth of ZIKV infection during the outbreak in six key French Polynesian archipelagos was constructed and studied by [136]. A nonlinear fractional-order model was proposed by [137] as a way to explain and grasp the

foot-and-mouth outbreaks. A fractional-order model for the spread and treatment of foot-and-mouth disease is presented and examined in [138]. Fractional order mathematical model to explain how the hand, foot, and mouth illness spreads [139]. The maximum principle of Pontryagin is used to derive the optimality control conditions. In [140] used a computer model to investigate the frequency of hand, foot, and mouth illness, a viral infectious disease. A time-delayed foot-and-mouth disease model that takes into account pertinent biological and ecological aspects, the effects of immunization, and disease carriers was given by [141].

4 Contribution of Fractional to Overcome the Impact of Disease

4.1 Ebola Model in Fractional Order with Caputo Derivative

Let's examine some of the main components of Ramos et al. [142]'s compartmental mathematical epidemic model and fractional order system is

$$\begin{cases} {}^{\mathfrak{C}}\mathbb{D}_{0,t}^{\upsilon_1,\upsilon_2} S(t) = \Lambda - (\beta_I I + \beta_H H + \beta_D D)\, S - (\tau+\mu)S, \\ {}^{\mathfrak{C}}\mathbb{D}_{0,t}^{\upsilon_1,\upsilon_2} E(t) = S(\beta_I I + \beta_H H + \beta_D D) - (\mu+\tau+\delta)E, \\ {}^{\mathfrak{C}}\mathbb{D}_{0,t}^{\upsilon_1,\upsilon_2} I(t) = \delta E - (\mu+\gamma)I, \\ {}^{\mathfrak{C}}\mathbb{D}_{0,t}^{\upsilon_1,\upsilon_2} H(t) = \gamma I - (\mu+\lambda+\alpha)H, \\ {}^{\mathfrak{C}}\mathbb{D}_{0,t}^{\upsilon_1,\upsilon_2} R(t) = \alpha H - (\mu+\tau)R, \\ {}^{\mathfrak{C}}\mathbb{D}_{0,t}^{\upsilon_1,\upsilon_2} D(t) = \lambda H - \theta D. \end{cases} \tag{30}$$

with

$$S(0) = S^0 \geq 0, H(0) = H^0 \geq 0, E(0) = E^0 \geq 0, I(0) = I^0 \geq 0, R(0) = R^0 \geq 0, D(0) = D^0 \geq 0. \tag{31}$$

There has been a mathematical investigation of the non-linear epidemiological model of Ebola virus sickness and therapy. To assess the effects of the fractional derivative on the treatment sections and ascertain the benefits of the parameters used in this Ebola dynamics model, several simulation tests depending on parameter values are carried out. By using fractal fractional derivative, the model produces numerical representations for a range of fractional values in accordance with the steady state point. Numerous numerical techniques can be used to analyze the end time value of a certain parameter in order to examine how different parameters affect the dynamics of the fractional order model.

Figures (1)-(6) illustrate graphs of approximations of solutions versus various fractional orders. As shown in Figures (1)-(6), as fractional values decrease, $S(t)$ and $R(t)$ increase, while $E(t)$,I(t), $H(t)$, and $D(t)$ decrease. The behaviour in all graphs changes when the fractional values are reduced, indicating that the roots will function more effectively if the fractional values are lower than the classical derivative. These simulations demonstrate how changes in value affect the model's behaviour. The simulation also shows how the health of Ebola patients may change over time. The significance of the research for forming judgements and setting boundaries thus grows. Different numerical techniques and the time fractional parameters are used to identify the mechanical characteristics of the fractional order model. The dynamics of the model have changed, according to simulations. With the aid of fractional values and discoveries from multiple dimensions, the findings of the nonlinear system memory were also identified. Without imposing any more requirements, it provides a better technique for how you want to manage the sickness. The numerical results show how the dynamics in the different fractional orders behave [143].

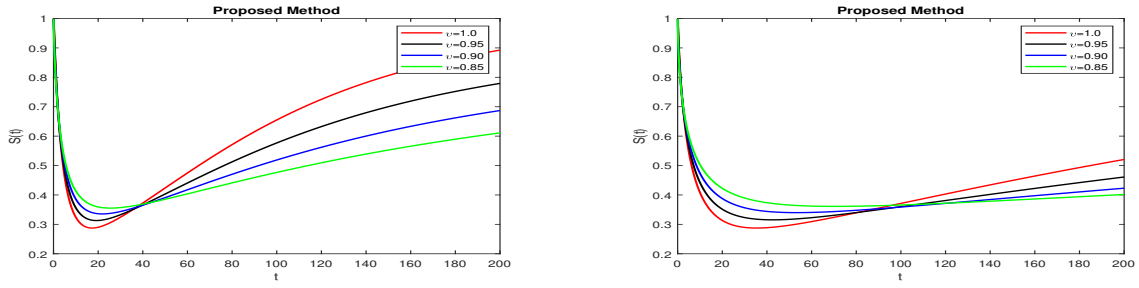

(a) At dimension 1 (b) At dimension 0.8

Fig. 1: $S(t)$ with Caputo fractional derivative

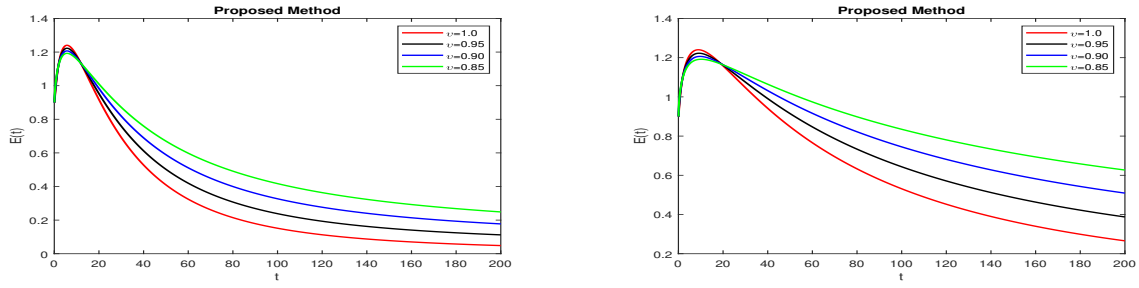

(a) At dimension 1 (b) At dimension 0.8

Fig. 2: $E(t)$ with Caputo fractional derivative

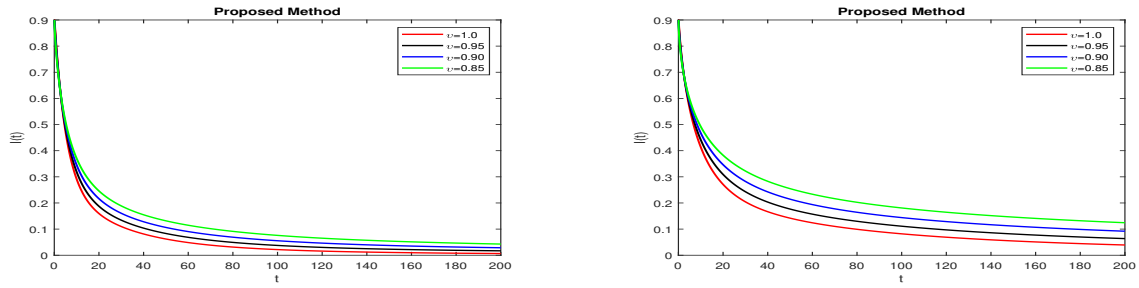

(a) At dimension 1 (b) At dimension 0.8

Fig. 3: $I(t)$ with Caputo fractional derivative

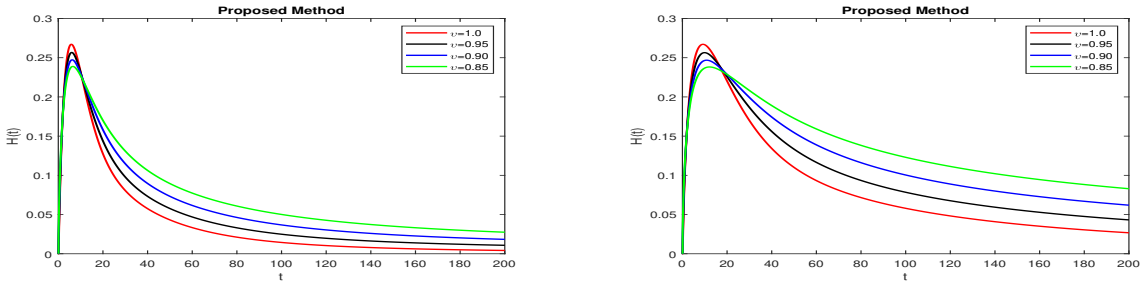

(a) At dimension 1 (b) At dimension 0.8

Fig. 4: $H(t)$ with Caputo fractional derivative

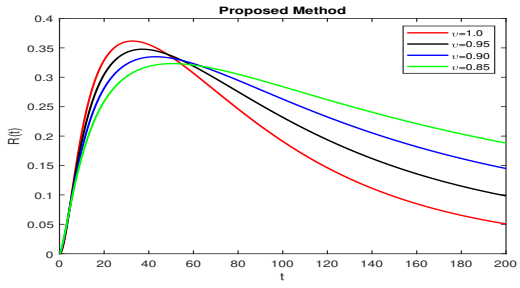

(a) At dimension 1

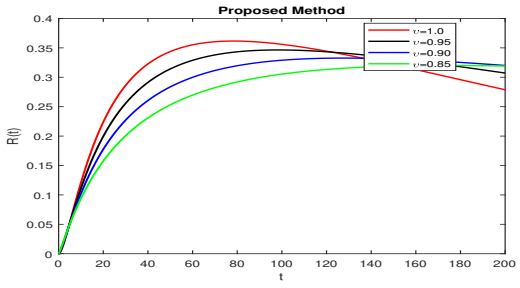

(b) At dimension 0.8

Fig. 5: $R(t)$ with Caputo fractional derivative

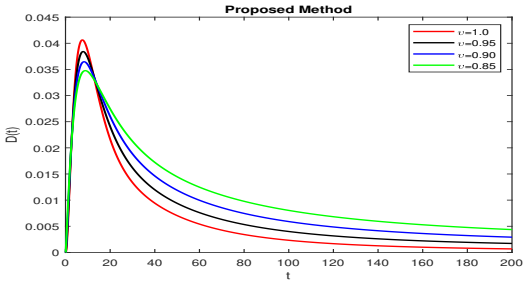

(a) At dimension 1

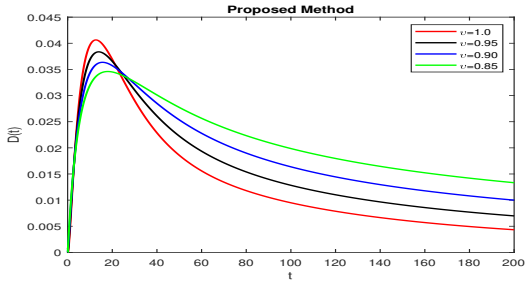

(b) At dimension 0.8

Fig. 6: $D(t)$ with Caputo fractional derivative

4.2 Omicron Variant with Caputo-Fabrizio Derivative

It is crucial to assess several approaches for COVID-19 infectious dynamics in the face of numerous intervention plans. A variety of analysts have created novel epidemic models for COVID-19 in a homogeneous host population utilizing a range of intervention tactics, as noted in [144], given the critical importance of intervention approaches.

$$
\begin{aligned}
{}^{\mathscr{CF}}\mathscr{D}^{\varpi}_{0,t}\mathbb{S} &= \overline{\ell_0} - \overline{\ell_1}\mathbb{S} - \frac{\overline{\ell_2}\mathbb{S}(\mathbb{I}+\overline{\ell_3}\mathbb{I}_{\mathfrak{I}})}{N} - \overline{\ell_4}\mathbb{S}\mathbb{M},\\
{}^{\mathscr{CF}}\mathscr{D}^{\varpi}_{0,t}\mathbb{E} &= \frac{\overline{\ell_2}\mathbb{S}(\mathbb{I}+\overline{\ell_3}\mathbb{I}_{\mathfrak{I}})}{N} + \overline{\ell_4}\mathbb{S}\mathbb{M} - (1-\overline{\ell_5})\overline{\ell_6}\mathbb{E} - \overline{\ell_5\ell_7}\mathbb{E} - \overline{\ell_1}\mathbb{E},\\
{}^{\mathscr{CF}}\mathscr{D}^{\varpi}_{0,t}\mathbb{I} &= (1-\overline{\ell_5})\overline{\ell_6}\mathbb{E} - (\overline{\ell_8}+\overline{\ell_1})\mathbb{I},\\
{}^{\mathscr{CF}}\mathscr{D}^{\varpi}_{0,t}\mathbb{I}_{\mathfrak{I}} &= \overline{\ell_5\ell_7}\mathbb{E} - (\overline{\ell_9}+\overline{\ell_1})\mathbb{I}_{\mathfrak{I}},\\
{}^{\mathscr{CF}}\mathscr{D}^{\varpi}_{0,t}\mathbb{R} &= \overline{\ell_8}\mathbb{I}(t) + \overline{\ell_9}\mathbb{I}_{\mathfrak{I}} - \overline{\ell_1}\mathbb{R},\\
{}^{\mathscr{CF}}\mathscr{D}^{\varpi}_{0,t}\mathbb{M} &= \overline{\ell_{10}}I + \overline{\ell_{11}}\mathbb{I}_{\mathfrak{I}} - \overline{\ell_1}\mathbb{M}.
\end{aligned}
\tag{32}
$$

The associated variables $\mathbb{S}$, $\mathbb{E}$, $\mathbb{I}$, $\mathbb{I}_{\mathfrak{I}}$, $\mathbb{R}$, $\mathbb{M}$ can be illustrated as susceptible, exposed, infected, asymptotically infected, recovered and reservoir persons. In case of parameters, $\overline{\ell_0}$, $\overline{\ell_1}$ represent birth and mortality rates,$\overline{\ell_2}$, $\overline{\ell_3}$, $\overline{\ell_4}$ describe the transmission coefficient, multiple, and disease transmission. $\overline{\ell_5}$ is an infection of asymptotic, parameter $\overline{\ell_6}$ show incubation, while $\overline{\ell_7}$ is infected transmission. Moreover, we illustrate the rate of recovery as $\overline{\ell_8}$, asymptotic persons as $\overline{\ell_9}$, while asymptotic and reservoir transmission pathogens are $\overline{\ell_{10}}, \overline{\ell_{11}}$ respectively. For the better representation of (32), we

simplify it by adding some constants.

$$
\begin{aligned}
{}^{\mathscr{CF}}\mathscr{D}^{\varpi}_{0,t}\mathbb{S} &= \overline{\ell_0} - \overline{\ell_1}\mathbb{S} - \overline{\ell_{13}}\mathbb{S}(\mathbb{I}+\overline{\ell_3}\mathbb{I}_{\mathfrak{D}}) - \overline{\ell_4}\mathbb{S}\mathbb{M},\\
{}^{\mathscr{CF}}\mathscr{D}^{\varpi}_{0,t}\mathbb{E} &= \overline{\ell_1}\mathbb{S} - \overline{\ell_{13}}\mathbb{S}(\mathbb{I}+\overline{\ell_3}\mathbb{I}_{\mathfrak{D}}) + \overline{\ell_4}\mathbb{S}\mathbb{M} + \overline{\ell_{14}}\mathbb{E} - \overline{\ell_{15}}\mathbb{E} - \overline{\ell_1}\mathbb{E},\\
{}^{\mathscr{CF}}\mathscr{D}^{\varpi}_{0,t}\mathbb{I} &= \overline{\ell_{14}}\mathbb{E} - \overline{\ell_{16}}\mathbb{I},\\
{}^{\mathscr{CF}}\mathscr{D}^{\varpi}_{0,t}\mathbb{I}_{\mathfrak{D}} &= \overline{\ell_{15}}\mathbb{E} - \overline{\ell_{17}}\mathbb{I}_{\mathfrak{D}},\\
{}^{\mathscr{CF}}\mathscr{D}^{\varpi}_{0,t}\mathbb{R} &= \overline{\ell_8}\mathbb{I} + \overline{\ell_9}\mathbb{I}_{\mathfrak{D}} - \overline{\ell_1}\mathbb{R},\\
{}^{\mathscr{CF}}\mathscr{D}^{\varpi}_{0,t}\mathbb{M} &= \overline{\ell_{10}}\mathbb{I} + \overline{\ell_{11}}\mathbb{I}_{\mathfrak{D}} - \overline{\ell_1}\mathbb{M},
\end{aligned}
\tag{33}
$$

with initial condition

$$\mathbb{S}(0)\geq 0,\ \mathbb{E}(0)\geq 0,\ \mathbb{I}(0)\geq 0,\ \mathbb{I}_{\mathfrak{D}}(0)\geq 0,\ \mathbb{R}(0)\geq 0,\ \mathbb{M}(0)\geq 0.$$

where $\overline{\ell_{13}} = \frac{\overline{\ell_2}}{N}$, $\overline{\ell_{14}} = (1-\overline{\ell_5})\overline{\ell_6}$, $\overline{\ell_{15}} = \overline{\ell_5\ell_7}$, $\overline{\ell_{16}} = \overline{\ell_8}+\overline{\ell_1}$ and $\overline{\ell_{17}} = \overline{\ell_9}+\overline{\ell_1}$. The numerical simulations describe the influences of ℓ = 0.85, 0.9, 0.95, 1.0 are shown in figure (7) which memory effect of fractional [145].

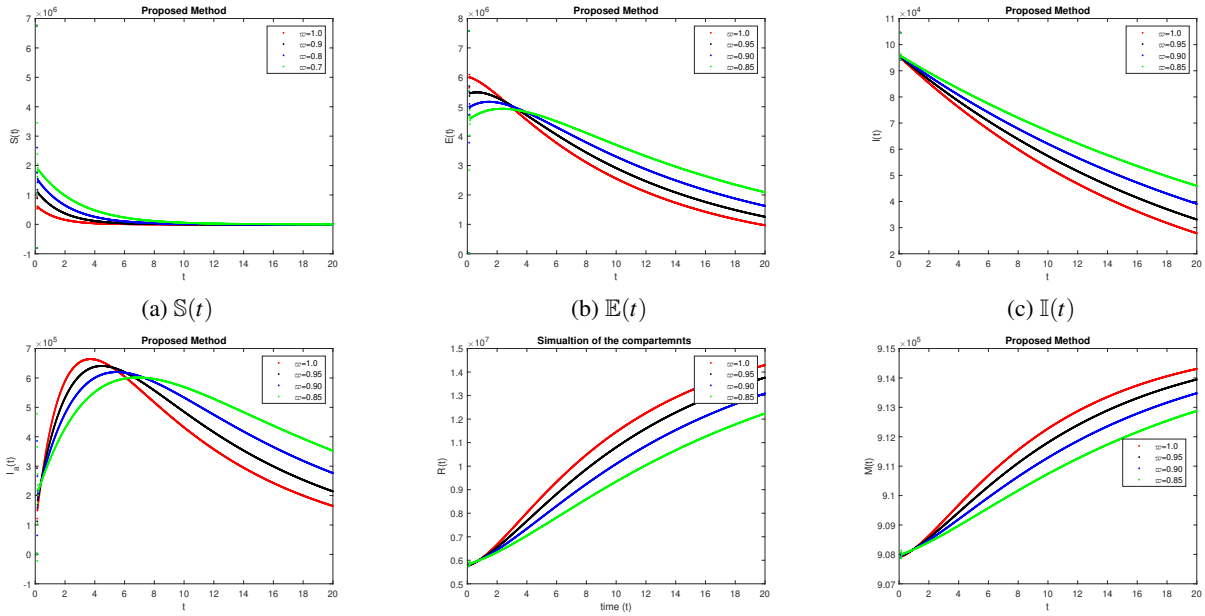

(a) $\mathbb{S}(t)$ (b) $\mathbb{E}(t)$ (c) $\mathbb{I}(t)$

(d) $\mathbb{I}_{\mathfrak{D}}(t)$ (e) $\mathbb{R}(t)$ (f) $\mathbb{M}(t)$

Fig. 7: Simulation of Compartments of Model with Caputo fractional derivative

4.3 Fractional-Order Bovine Babesiosis Disease with ABC

classical model is modified in [146], we have subsequent fractional order model in time t

$$
\begin{aligned}
D^{\beta}U &= (\mu_B+\alpha)(1-U-V) - \beta_B UZ,\\
D^{\beta}V &= \beta_B UZ - \lambda_B V,\\
D^{\beta}Z &= \beta_T(1-Z)V - \mu_T pZ,
\end{aligned}
\tag{34}
$$

with initial constraints $U(0)=0.4, V(0)=0.5, Z(0)=0.6$

The analytical solution of the fractional differential equation was given as a nonlinear system utilizing the Caputo and ABC derivative. With starting values of $U(0) = 0.4$, $V(0) = 0.5$, and $Z(0) = 0.6$, we represent $U(t)$, $V(t)$, and $Z(t)$ in this model. Figure (8) illustrates the numerical outcomes of $U(t)$, $V(t)$, and $Z(t)$ for various fractional estimations of β obtained by utilizing Caputo and ABC fractional derivative. Numerical simulations of an updated epidemic model with arbitrary order have been used to show the correlation between fractional order and relaxation time. This discovery provides important details about the use of fractional order modelling to the dynamics of the babesiosis disease and tick population. [147].

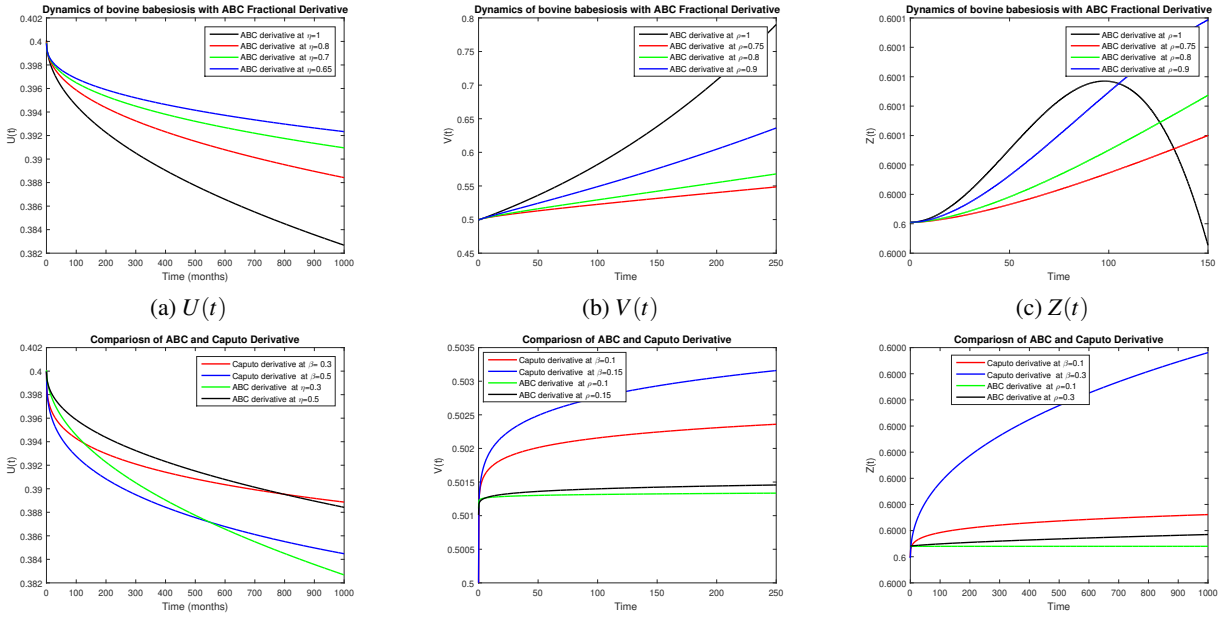

(a) $U(t)$ (b) $V(t)$ (c) $Z(t)$

(d) $U(t)$ (e) $V(t)$ (f) $Z(t)$

Fig. 8: Simulation of Compartments of Model with ABC fractional derivative

4.4 Measles Epidemic Model with Hybrid Operator (Constant Proportional with Caputo, Caputo Fabrizio, ABC)

Here, we give the measles transmission dynamics model citation 171 in terms of a time-fractional order variant. The model is divided into six sections: The letters **S** stand for susceptible individuals, **V** for persons who have received vaccinations, **E** for the exposed area, **I** for infected individuals, **T** for those who have received treatment, and **R** for those who have recovered from infection. The above description can be expressed as a set of differential equations of time-fractional order, as shown below:

$$\begin{cases} {}^{CPC}_{0}\mathrm{D}_t^{\eta}\mathbf{S}(t) = (1-\varepsilon)\rho + (1-\gamma_2)\alpha\mathbf{V} - (\gamma_1+\omega)\mathbf{S} - \frac{\beta\nu_{\mathbf{I}}}{\mathbf{N}}\mathbf{SI} - \frac{\beta\nu_{\mathbf{T}}}{\mathbf{N}}\mathbf{ST}, \\ {}^{CPC}_{0}\mathrm{D}_t^{\eta}\mathbf{V}(t) = \varepsilon\rho - \big(\omega + (1-\gamma_2)\alpha\big)\mathbf{V} + \gamma_1\mathbf{S}, \\ {}^{CPC}_{0}\mathrm{D}_t^{\eta}\mathbf{E}(t) = \frac{\beta\nu_{\mathbf{I}}}{\mathbf{N}}\mathbf{SI} + \frac{\beta\nu_{\mathbf{T}}}{\mathbf{N}}\mathbf{ST} - (\gamma_3+\omega+\mu)\mathbf{E}, \\ {}^{CPC}_{0}\mathrm{D}_t^{\eta}\mathbf{I}(t) = \mu\mathbf{E} - (\gamma_4+\omega+\delta_{\mathbf{I}})\mathbf{I}, \\ {}^{CPC}_{0}\mathrm{D}_t^{\eta}\mathbf{T}(t) = \gamma_4\mathbf{I} - (\omega+\delta_{\mathbf{T}})\mathbf{T}, \\ {}^{CPC}_{0}\mathrm{D}_t^{\eta}\mathbf{R}(t) = \gamma_3\mathbf{E} + \delta_{\mathbf{I}}\mathbf{I} + \delta_{\mathbf{T}}\mathbf{T} - \omega\mathbf{R}. \end{cases} \tag{35}$$

with non-negative initial constraints,

$$\mathbf{S}(0) = \mathbf{S}^0, \mathbf{V}(0) = \mathbf{V}^0, \mathbf{E}(0) = \mathbf{E}^0, \mathbf{I}(0) = \mathbf{I}^0, \mathbf{T}(0) = \mathbf{T}^0, \mathbf{R}(0) = \mathbf{R}^0 \tag{36}$$

where, A composite measurement called $\beta \geq 0$ assesses both the rate of contact and the possibility of transmission. $\nu_{\mathbf{I}}$ and $\nu_{\mathbf{T}}$, respectively, measure the reduction in transmissibility of infected and treated individuals who do not finish therapy compared to infectious individuals. ε is the percentage of newcomers to the community who are immunised or have

parental immunity, α is the rate at which a vaccine loses its efficacy after a single dose, ω is the natural fatality rate, μ is the rate at which unprotected people become infected, γ_1 and γ_2 displays the proportion of vaccine recipients who receive the second dose of the vaccine, γ_3 represents the measles therapy rate, and γ_4 represents the treatment rate for infected individuals. The natural restorable rate for infected people is $\delta_{\mathbf{I}}$, whereas the recovery rate for people who have received treatment is $\delta_{\mathbf{T}}$. All of the metrics should be positive and backed by biological factors.

The simulation of the taken into consideration version is depicted inside the figures in this phase by using parameter's values from [148] are are $\varepsilon = 0.250$, $\rho = 0.950$, $\alpha = 0.1$, $\gamma_1 = 0.15$, $\gamma_2 = 0.1$, $\gamma_3 = 0.08$, $\gamma_4 = 0.05$, $\omega = 0.0069$, $\mu = 0.678, 0.885$, $\delta_{\mathbf{I}} = 0.04762$, $\delta_{\mathbf{T}} = 0.136$, $\beta = 0.03739, 0.575$, $\nu_{\mathbf{I}} = 0.913$, and $\nu_{\mathbf{T}} = 0.978$. Those simulations demonstrate how variations in value have an effect at the model's behavior. We have employed initial points as $\mathbf{S}_0 = 45$, $\mathbf{V}_0 = 15$, $\mathbf{E}_0 = 10$, $\mathbf{I}_0 = 20$, $\mathbf{T}_0 = 5$ and $\mathbf{R}_0 = 5$ such that the total population under examination is $\mathbf{N} = 100$. The series result with CPC operator according to distinct values of η is simulated in Figures (9)-(10) for both the $\mathbb{R}^0 < 1$ and $\mathbb{R}^{star} > 1$, while the series result with CPABC operator according to distinct values of η is simulated in Figures (11)-(12) for both the $\mathbb{R}^0 < 1$ and $\mathbb{R}^\star > 1$, and the series result with CPCF operator according to distinct values of η is simulated in Figures (13)-(14) for both the $\mathbb{R}^0 < 1$ and $\mathbb{R}^\star > 1$, using MATLAB. The simulations of measles epidemic model for $\mathbb{R}^0 < 1$ with CPC and CPABC operators demonstrated in Figure (9) and (11) respectively, for distinct values of fractional order η show all the compartments converging to their disease free equilibrium. While Figures (10) and (12) describe the endemic case $\mathbb{R}^\star > 1$. We have used different values of fractional order $\eta = 0.95$, $\eta = 0.90$, $\eta = 0.85$ and $\eta = 0.80$. Fractional order derivations, which might be the most outstanding and dependable compared to classical order, had been shown to be greater efficient in explaining bodily approaches. In contrast, those operators are extra worthwhile than current non-integer order fashions. To track the end time value of the given parameter and look at how various factors have an effect on the dynamics of the fractional order version, an expansion of numerical strategies may be used. The supplied numerical results represent the conduct of the dynamics that may be observed within the one-of-a-kind fractal orders.

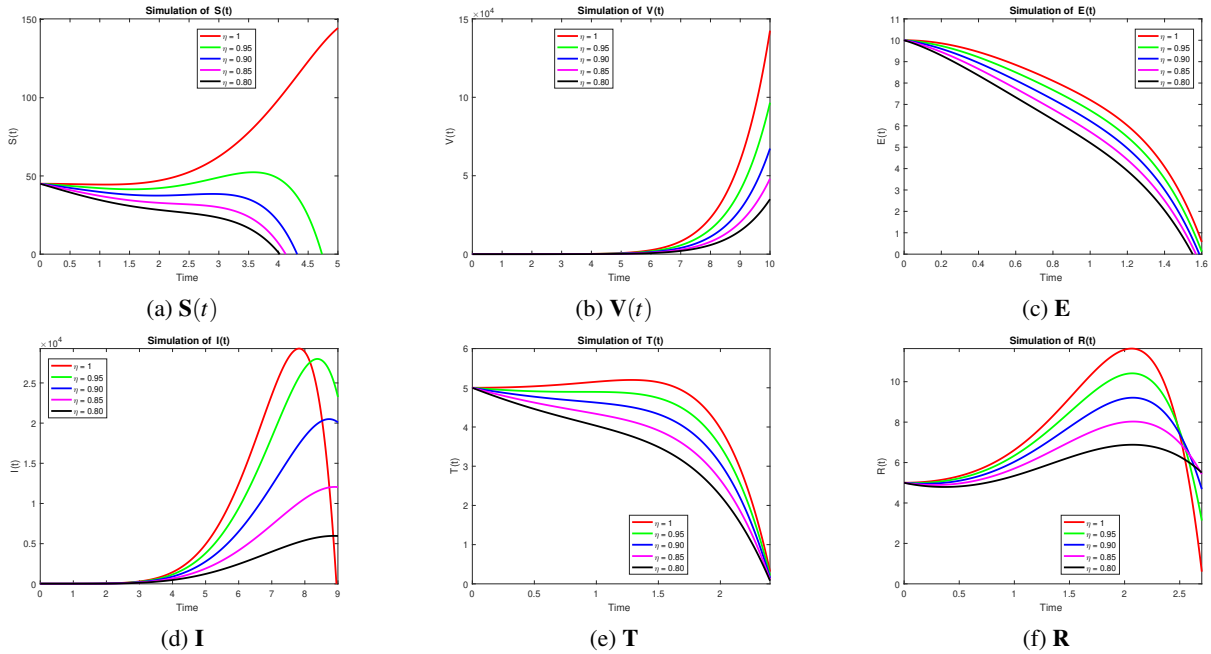

(a) $\mathbf{S}(t)$ (b) $\mathbf{V}(t)$ (c) $\mathbf{E}$

(d) $\mathbf{I}$ (e) $\mathbf{T}$ (f) $\mathbf{R}$

Fig. 9: Simulation of transmission dynamics of Measles epidemic for $\mathbb{R}^0 < 1$ with CPC

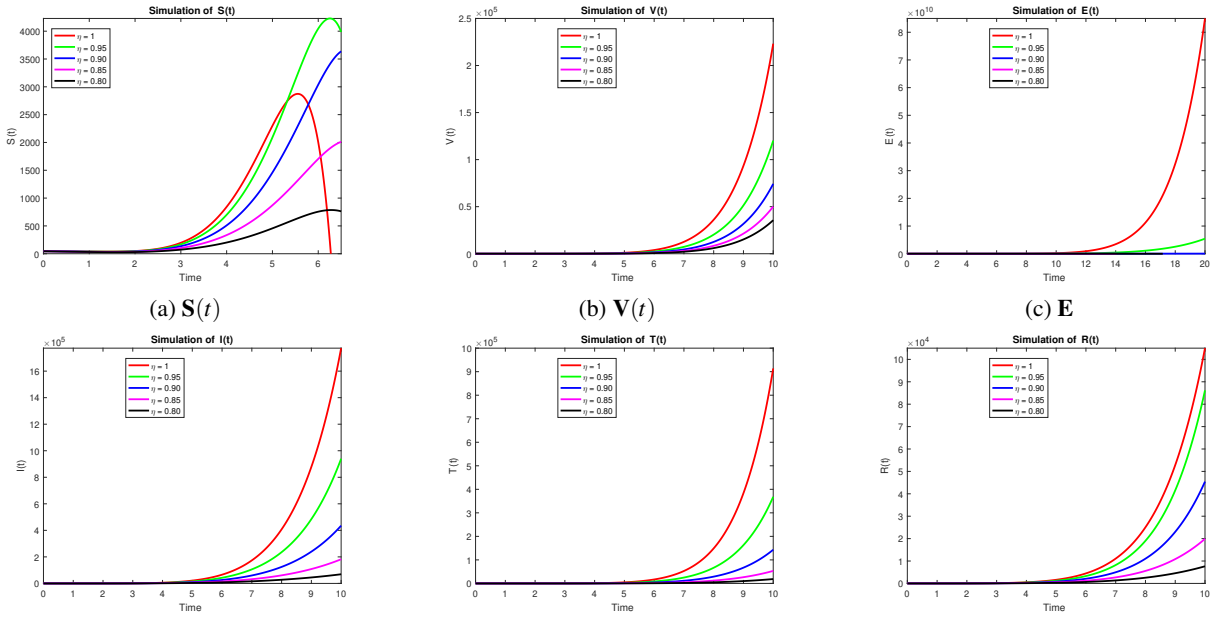

(a) $\mathbf{S}(t)$ (b) $\mathbf{V}(t)$ (c) $\mathbf{E}$

(d) $\mathbf{I}$ (e) $\mathbf{T}$ (f) $\mathbf{R}$

Fig. 10: Simulation of transmission dynamics of Measles epidemic for $\mathbb{R}^0 > 1$ with CPC

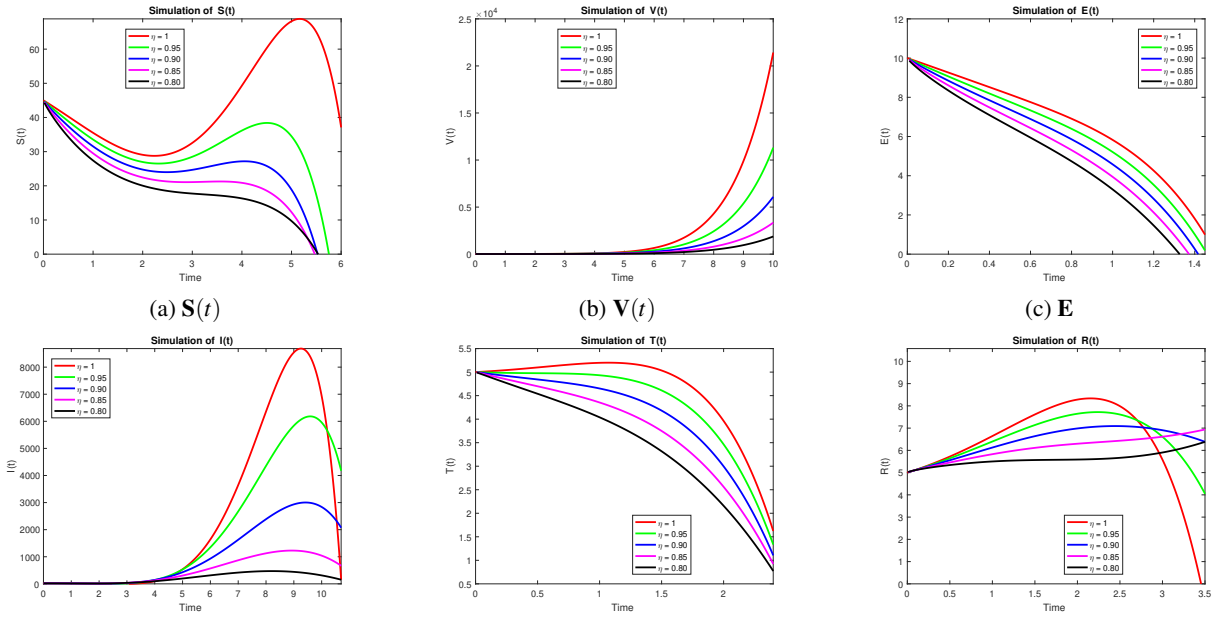

(a) $\mathbf{S}(t)$ (b) $\mathbf{V}(t)$ (c) $\mathbf{E}$

(d) $\mathbf{I}$ (e) $\mathbf{T}$ (f) $\mathbf{R}$

Fig. 11: Simulation of transmission dynamics of Measles epidemic for $\mathbb{R}^0 < 1$ with CPABC

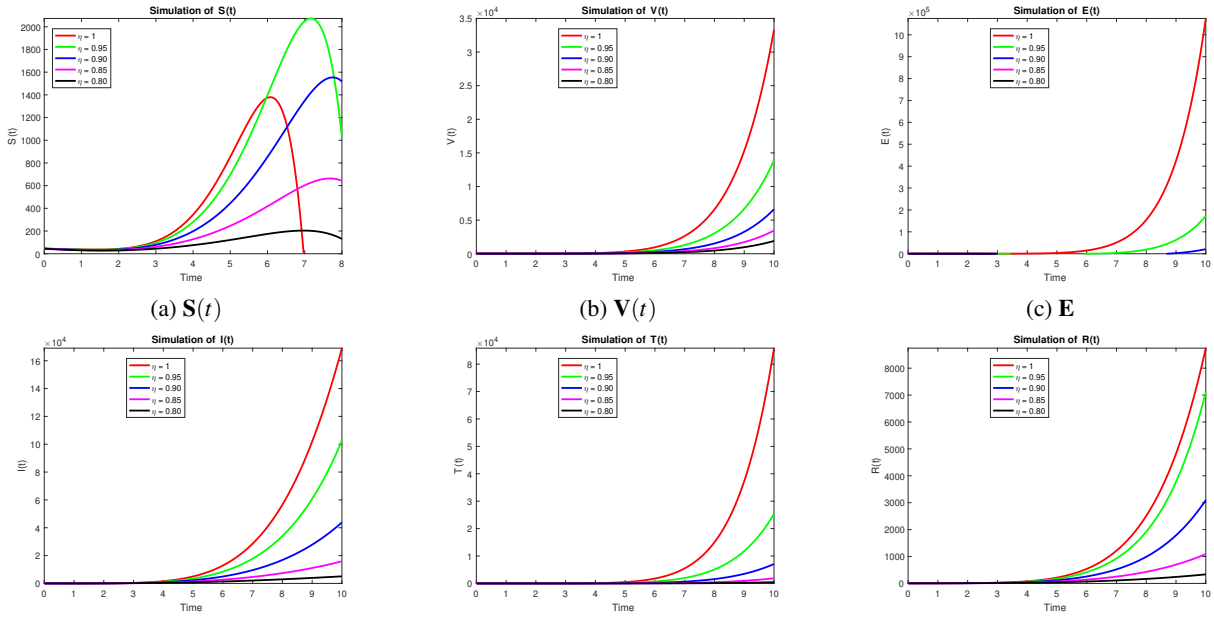

(a) $\mathbf{S}(t)$ (b) $\mathbf{V}(t)$ (c) $\mathbf{E}$

(d) $\mathbf{I}$ (e) $\mathbf{T}$ (f) $\mathbf{R}$

Fig. 12: Simulation of transmission dynamics of Measles epidemic for $\mathbb{R}^0 > 1$ with CPABC

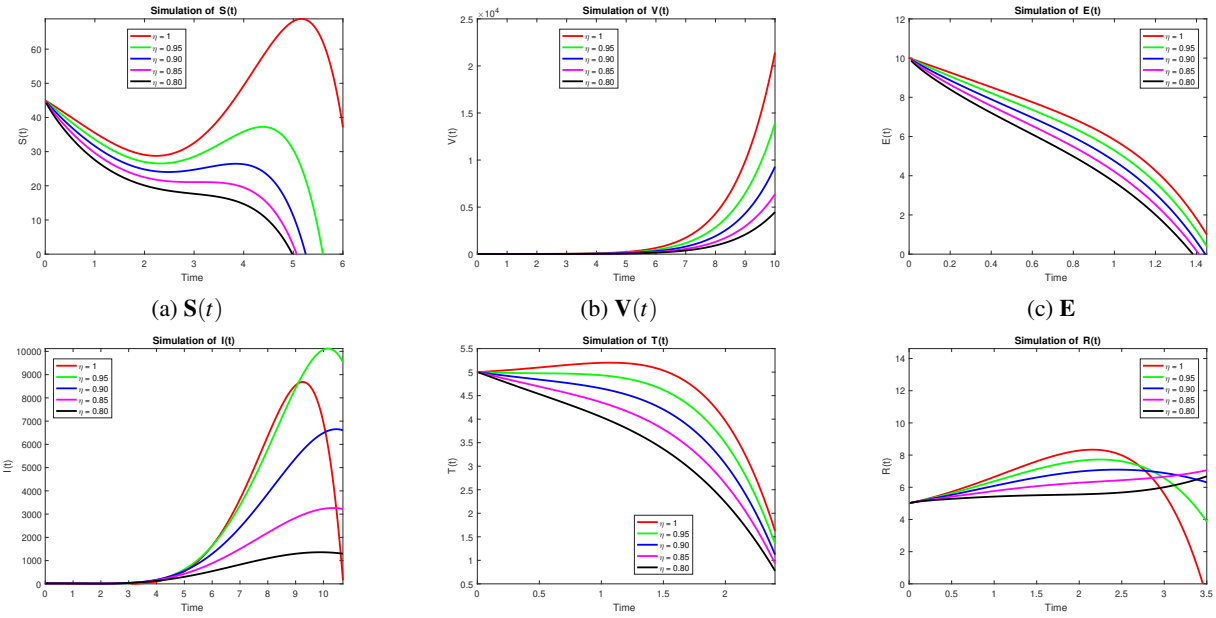

(a) $\mathbf{S}(t)$ (b) $\mathbf{V}(t)$ (c) $\mathbf{E}$

(d) $\mathbf{I}$ (e) $\mathbf{T}$ (f) $\mathbf{R}$

Fig. 13: Simulation of transmission dynamics of Measles epidemic for $\mathbb{R}^0 < 1$ with CPCF

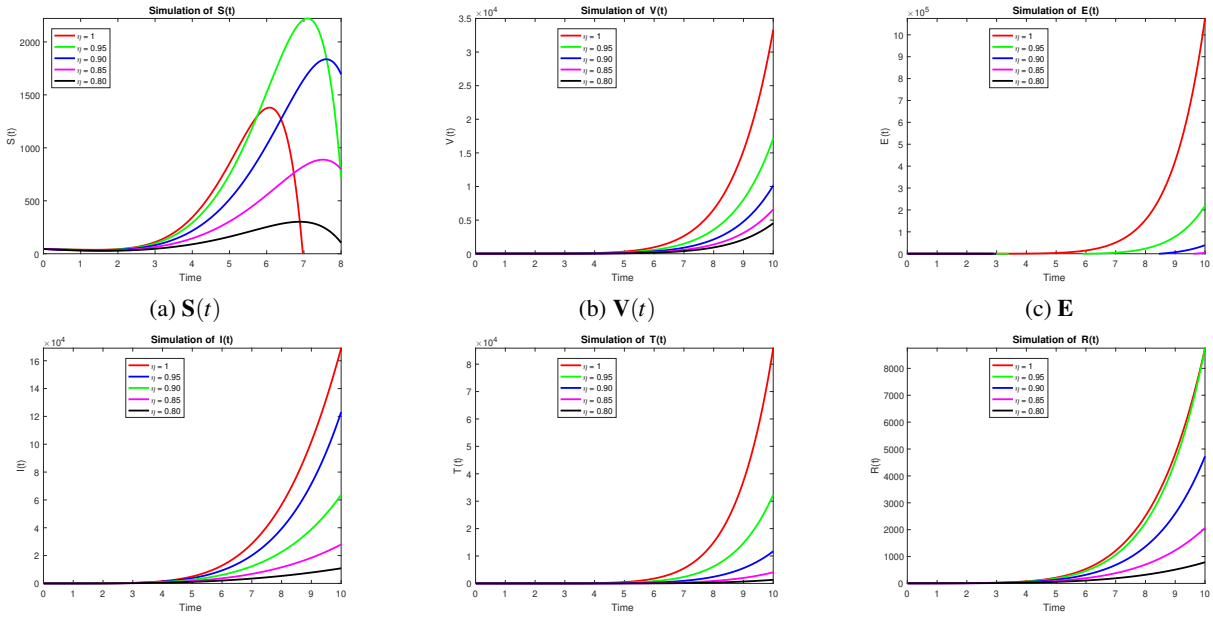

(a) $\mathbf{S}(t)$ (b) $\mathbf{V}(t)$ (c) $\mathbf{E}$

(d) $\mathbf{I}$ (e) $\mathbf{T}$ (f) $\mathbf{R}$

Fig. 14: Simulation of transmission dynamics of Measles epidemic for $\mathbb{R}^0 > 1$ with CPCF

5 Fractional Order Application on Epidemic Model

New fractional operators, the infectious disease model has been studied in this paper. The mechanical features of the fractional order model are discovered using various numerical methods and time-dependent fractional parameters. Presence and originality have been proven. The model's local and global stability analysis has been found. Numerical simulations are performed for the proposed method in the spectrum of fractional order to demonstrate the consequences of fractional and fractal orders as a way to support the theoretical findings. We used an exceptionally effective numerical strategy to get the model and simulation' answers. Also, we present conditions of existence for a solution to the purposed epidemic model and to calculate the reproduction number in certain state conditions of the analyzed dynamic system. Infectious disease fractional order model is offered for analysis with simulations in order to determine the possible efficacy of disease transmission in the Community. For this reason, we employed the proposed fractal fractional derivative model in the example of Wuhan, China, with the given beginning conditions. In conclusion, again the mathematical models with fractional operators can facilitate the improvement of the decisions making for the measures in management of an epidemic situation. Here are the fractional differential equations that are used in the compartmental mathematical epidemic model proposed by Parsamanesh et al. [149] to clarify how viruses spread:

$$\begin{cases} {}^{CF}_{0}D^{\alpha}_{t}S(t) = (1-q)\Lambda - \frac{\beta SI}{N} - (\mu+p)S + \gamma I + \varepsilon V, \\ {}^{CF}_{0}D^{\alpha}_{t}I(t) = \frac{\beta SI}{N} - (\mu+\gamma+\alpha)I, \\ {}^{CF}_{0}D^{\alpha}_{t}V(t) = q\Lambda + pS - (\mu+\varepsilon)V. \end{cases} \tag{37}$$

where the initial conditions are

$$S(0) = S^0 \geq 0, I(0) = I^0 \geq 0, V(0) = V^0 \geq 0. \tag{38}$$

Where $S(t)$ stand for the susceptible group of population over time t, $I(t)$ stand for the infected group of population over time t and $V(t)$ stand for the vaccinated group of population over time t. The parameters of the proposed model are define in table 1.

Table 1: Parameters details of Model

Parameters	Definitions
μ	Natural Mortality Rate
β	Contact Rate
γ	Treatment Rate
ε	Losing Immunity Rate
q	Vaccination Rate in Newcomers individuals
p	Vaccination Rate in Susceptible individuals
Λ	population per unit of time, which could include new immigrants or babies
α	The hypothetical scenario also includes a rate of death due to diseases.
N	Total Population

The total population is

$$\mathbb{N}(t) = S(t) + I(t) + V(t). \tag{39}$$

5.1 Positiveness and Boundedness of Solutions

Lemma 1. *Let initial conditions be*

$$\left\{S^0, I^0, V^0\right\} \subset \Psi. \tag{40}$$

Then if the solutions $\{S, I, V\}$ *exist, they are all positive for all* $t > 0$

Proof. For proof, consider I.

$$ {}_0^{CF}D_t^{\alpha} I(t) = \frac{\beta SI}{N} - (\mu + \gamma + \alpha)I, \tag{41}$$

So,

$$S \geq 0.$$

Therefore

$$ {}_0^{CF}D_t^{\alpha} I(t) = -\{(\mu + \gamma + \alpha)\}I, \tag{42}$$

which in turn leads to

$$I(t) \geq I(0)e^{-\{(\mu+\gamma+\alpha)\}t}. \tag{43}$$

This shows that $I(t)$ is positive for $\forall t \geq 0$. On the other hand, we have that

$$I(t) \geq 0. \tag{44}$$

In case of $V(t)$

$$ {}_0^{CF}D_t^{\alpha} V(t) = q\Lambda + pS - (\mu + \varepsilon)V, \tag{45}$$

We get

$$S \geq 0.$$
$$V(t) \geq -(\mu + \varepsilon)V.$$

This leads to

$$V(t) \geq V(0)e^{-(\mu+\varepsilon)t},$$

which shows that $V(t)$ is positive for $\forall t \geq 0$. On the other hand

$$ {}_0^{CF}D_t^{\alpha} V(t) \leq q\Lambda + pS. \tag{46}$$

Having the norms, i.e

$$\|\Xi\|_{\infty} = \max_{t \in D_f} |\Xi(t)|. \tag{47}$$

It is essential to note that due to the system's biological soundness.

$$\|S\|_{\infty}, \qquad \|I\|_{\infty}, \qquad \|V\|_{\infty}, \qquad < \infty \qquad \forall t \geq 0. \tag{48}$$

$$ {}_0^{CF}D_t^{\alpha} V(t) \leq q\Lambda + p\|S\|_{\infty}. \tag{49}$$

Theorem 1. *Assuming that a function $\Phi(t)$ is continuous and bounded for $t \in [0,\infty[$, then for $0 < \alpha \leq 1$.*

$$\lim_{t\to\infty} \frac{1}{t^{\alpha+1}\Gamma(\alpha)} \int_0^t \Phi(\vartheta)(t-\vartheta)^{\alpha-1} d\vartheta = 0. \tag{50}$$

Proof. For proof, since $\Phi(t)$ is continuous and bounded, then for all $t \in [0,\infty[$ there exists $K < \infty$ such that $\|\Phi\|_\infty = \sup_{t\in D_t} |\Phi(t)| < K$.

$$\lim_{t\to\infty} \frac{1}{t^{\alpha+1}\Gamma(\alpha)} \int_0^t \Phi(\vartheta)(t-\vartheta)^{\alpha-1} d\vartheta \leq \lim_{t\to\infty} \frac{1}{t^{\alpha+1}\Gamma(\alpha)} \int_0^t |\Phi(\vartheta)|(t-\vartheta)^{\alpha-1} d\vartheta, \tag{51}$$

$$\leq \lim_{t\to\infty} \frac{1}{t^{\alpha+1}\Gamma(\alpha)} \int_0^t \sup_{\eta\in(0,\vartheta)} |\Phi(\eta)|(t-\vartheta)^{\alpha-1} d\vartheta,$$

$$\leq \lim_{t\to\infty} \frac{\|\Phi\|_\infty}{t^{\alpha+1}\Gamma(\alpha)} \int_0^t (t-\vartheta)^{\alpha-1} d\vartheta,$$

$$\leq \lim_{t\to\infty} \frac{K}{t\Gamma(\alpha+1)} = 0. \tag{52}$$

We now assume that $\Phi(t)$ is bounded, then

$$\|\Phi\|_\infty = \sup_{t\in D_\Phi} |\Phi(t)| < K < \infty. \tag{53}$$

We define as

$${}^C\langle\Phi(t)\rangle^{\alpha,\kappa_1} = \frac{1}{t^\alpha\Gamma(\alpha)} \int_0^t \Phi(\vartheta)(t-\vartheta)^{\alpha-1} d\vartheta, \tag{54}$$

then

$${}^C\langle\Phi(t)\rangle^{\alpha,\kappa_1} \leq \left|{}^C\langle\Phi(t)\rangle^{\alpha,\kappa_1}\right| \leq \frac{1}{t^\alpha\Gamma(\alpha)} \int_0^t |\Phi(\vartheta)|(t-\vartheta)^{\alpha-1} d\vartheta,$$

$$\leq \frac{K}{t^\alpha\Gamma(\alpha+1)} t^\alpha,$$

$$\leq \frac{K}{\Gamma(\alpha+1)},$$

Now, we consider the class $S(t)$

$$\begin{aligned} S(t) - S(0) = \frac{1}{\Gamma(\alpha)} \int_0^t \left((1-q)\Lambda - \frac{\beta SI}{N} - (\mu+p)S + \gamma I + \varepsilon V\right) \\ + \frac{\sigma_1}{\Gamma(\alpha)} \int_0^t S(\vartheta)(t-\vartheta)^{\alpha-1} dB_1\vartheta. \end{aligned} \tag{55}$$

Dividing by t^α, so we have

$$\begin{aligned} \frac{S(t)-S(0)}{t^\alpha} &= \frac{1}{t^\alpha\Gamma(\alpha)} \int_0^t \left((1-q)\Lambda - \frac{\beta SI}{N} - (\mu+p)S + \gamma I + \varepsilon V\right) \\ &\quad + \frac{\sigma_1}{t^\alpha\Gamma(\alpha)} \int_0^t S(\vartheta)(t-\vartheta)^{\alpha-1} dB_1\vartheta. \\ &= \frac{(1-q)\Lambda}{\Gamma(\alpha+1)} - \beta^C\langle\frac{SI}{N}\rangle^\alpha - (\mu+p)^C\langle S\rangle^\alpha + \gamma^C\langle I\rangle^\alpha + \varepsilon^C\langle V\rangle^\alpha \\ &\quad + \frac{\sigma_1}{t^\alpha\Gamma(\alpha)} \int_0^t S(\vartheta)(t-\vartheta)^{\alpha-1} dB_1\vartheta, \\ {}^C\langle S\rangle^\alpha &= \frac{(1-q)\Lambda}{\Gamma(\alpha+1)(\mu+p)} + \frac{1}{(\mu+p)}\Big[-\frac{S(t)-S(0)}{t^\alpha} - \beta^C\langle\frac{SI}{N}\rangle^\alpha + \gamma^C\langle I\rangle^\alpha + \varepsilon^C\langle V\rangle^\alpha \\ &\quad + \frac{\sigma_1}{t^\alpha\Gamma(\alpha)} \int_0^t S(\vartheta)(t-\vartheta)^{\alpha-1} dB_1\vartheta\Big]. \end{aligned} \tag{56}$$

Then, we have

$$\lim_{t\to\infty} {}^{C}\langle S\rangle^{\alpha} = \frac{(1-q)\Lambda}{\Gamma(\alpha+1)(\mu+p)}. \tag{57}$$

We consider the class I, we have the following

$$\begin{aligned} I(t)-I(0) &= \frac{1}{\Gamma(\alpha)}\int_0^t \left(\frac{\beta SI}{N}-(\mu+\gamma+\alpha)I\right) \\ &+ \frac{\sigma_2}{\Gamma(\alpha)}\int_0^t I(\vartheta)(t-\vartheta)^{\alpha-1}dB_2\vartheta, \end{aligned} \tag{58}$$

and dividing by t^{α} yields

$$\begin{aligned} \frac{I(t)-I(0)}{t^{\alpha}} &= \frac{1}{t^{\alpha}\Gamma(\alpha)}\int_0^t \left(\frac{\beta SI}{N}-(\mu+\gamma+\alpha)I\right) \\ &+ \frac{\sigma_2}{t^{\alpha}\Gamma(\alpha)}\int_0^t I(\vartheta)(t-\vartheta)^{\alpha-1}dB_2\vartheta, \end{aligned}$$

$${}^{C}\langle I\rangle^{\alpha} = \frac{\beta}{(\mu+\gamma+\alpha)}\,{}^{C}\langle\frac{SI}{N}\rangle^{\alpha} + \frac{1}{(\mu+\gamma+\alpha)}\Big[-\frac{I(t)-I(0)}{t^{\alpha}} + \frac{\sigma_2}{t^{\alpha}\Gamma(\alpha)}\int_0^t I(\vartheta)(t-\vartheta)^{\alpha-1}dB_2\vartheta\Big],$$

so

$$\lim_{t\to\infty} {}^{C}\langle I\rangle^{\alpha} = 0. \tag{59}$$

We consider the class V, we have the following

$$\begin{aligned} V(t)-V(0) &= \frac{1}{\Gamma(\alpha)}\int_0^t (q\Lambda+pS-(\mu+\varepsilon)V) \\ &+ \frac{\sigma_3}{\Gamma(\alpha)}\int_0^t V(\vartheta)(t-\vartheta)^{\alpha-1}dB_3\vartheta, \end{aligned} \tag{60}$$

and dividing by t^{α} yields

$$\begin{aligned} \frac{V(t)-V(0)}{t^{\alpha}} &= \frac{1}{t^{\alpha}\Gamma(\alpha)}\int_0^t (q\Lambda+pS-(\mu+\varepsilon)V) \\ &+ \frac{\sigma_3}{t^{\alpha}\Gamma(\alpha)}\int_0^t V(\vartheta)(t-\vartheta)^{\alpha-1}dB_3\vartheta, \end{aligned}$$

$$\begin{aligned} \frac{V(t)-V(0)}{t^{\alpha}} &= \frac{q\Lambda}{\Gamma(\alpha+1)} + p\,{}^{C}\langle S\rangle^{\alpha} - (\mu+\varepsilon)\,{}^{C}\langle V\rangle^{\alpha} \\ &+ \frac{\sigma_3}{t^{\alpha}\Gamma(\alpha)}\int_0^t V(\vartheta)(t-\vartheta)^{\alpha-1}dB_3\vartheta, \end{aligned}$$

$${}^{C}\langle V\rangle^{\alpha} = \frac{q\Lambda}{(\mu+\varepsilon)\Gamma(\alpha+1)} + \frac{1}{(\mu+\varepsilon)}\Big[-\frac{V(t)-V(0)}{t^{\alpha}} + p\,{}^{C}\langle S\rangle^{\alpha} + \frac{\sigma_3}{t^{\alpha}\Gamma(\alpha)}\int_0^t V(\vartheta)(t-\vartheta)^{\alpha-1}dB_3\vartheta\Big]$$

so

$$\lim_{t\to\infty} {}^{C}\langle V\rangle^{\alpha} = \frac{q\Lambda}{(\mu+\varepsilon)\Gamma(\alpha+1)}.$$

Therefore, we write

$$\lim_{t\to\infty} {}^{C}\langle S\rangle^{\alpha} = \frac{(1-q)\Lambda}{\Gamma(\alpha+1)(\mu+p)}. \tag{61}$$

$$\lim_{t\to\infty} {}^{C}\langle I\rangle^{\alpha} = 0. \tag{62}$$

$$\lim_{t\to\infty} {}^{C}\langle V\rangle^{\alpha} = \frac{q\Lambda}{(\mu+\varepsilon)\Gamma(\alpha+1)}. \tag{63}$$

Theorem 2. *Epidemic infectious model (37) solution is distinct and constrained in R^3_+ according to initial conditions.*

Proof. We control it by

$$\begin{cases} {}^{CF}_{0}D^{\alpha}_{t}S(t)\Big|_{S=0} = (1-q)\Lambda + \gamma I + \varepsilon V \geq 0, \\ {}^{CF}_{0}D^{\alpha}_{t}I(t)\Big|_{I=0} \geq 0, \\ {}^{CF}_{0}D^{\alpha}_{t}V(t)\Big|_{V=0} = q\Lambda + pS \geq 0. \end{cases} \tag{64}$$

According to equation (64), the solution cannot escape the hyper plane if $\{S(0);I(0);V(0)\} \in R^3_+$, hence proved.

5.2 Well Posedness of the Model and Biological Feasibility

In this section we show that model is well-posedness and solution in feasible region for all t. We have

$${}^{CF}_{0}D^{\alpha}_{t}N(t) = \Lambda - \mu N - \alpha I. \tag{65}$$

So in the absence of disease, then

$${}^{CF}_{0}D^{\alpha}_{t}N(t) = \Lambda - \mu N. \tag{66}$$

We want that the function $N(t)$ is a positively increasing function $\frac{dN}{dt} > 0$

$${}^{CF}_{0}D^{\alpha}_{t}N(t) \geq N(t) < \frac{\Lambda}{\mu}. \tag{67}$$

It has

$$\Omega = \left\{ (S,I,V) \in R^3_+ : S+I+V = N(t) < \frac{\Lambda}{\mu} \right\}. \tag{68}$$

Here, R^3_+ is the positive cone of R^3_+, which also includes its faces in the lower dimensions.

5.3 Analysis of Equilibrium Points and Sensitivity Analysis

By using the system (37), the system has two solutions, when $I = 0$, the disease free equilibrium points E^0 is
$E^0 = (S^0, I^0, V^0)$, where $S^\star = \frac{\Lambda(\mu(1-q)+\varepsilon)}{\mu(\mu+\varepsilon+p)}, I^\star = 0, V^\star = \frac{\Lambda(\mu q+p)}{\mu(\mu+\varepsilon+p)}$.
When $I > 0$, the endemic equilibrium points $E^\star = (S^\star, I^\star, V^\star)$, where
$S^\star = \frac{\Lambda(\mu+\gamma+\alpha)}{\beta\mu}\left\{1 - \frac{\alpha(\mathscr{R}_0-1)}{\mu\mathscr{R}_0+\alpha(\mathscr{R}_0-1)}\right\}, I^\star = \frac{\Lambda(\mathscr{R}_0-1)}{\mu\mathscr{R}_0+\alpha(\mathscr{R}_0-1)}$,
and
$V^\star = \frac{q\Lambda}{\mu+\varepsilon}\left\{1 - \frac{p(\mu+\alpha q+\varepsilon)}{q(\mu+p+\varepsilon)\{\mu\mathscr{R}_0+\alpha(\mathscr{R}_0-1)\}}\right\}$.
The reproductive number $\mathscr{R}_0$ details given in [150], we have

$$\mathscr{R}_0 = \frac{\beta(\mu(1-q)+\varepsilon)}{(\mu+\gamma+\alpha)(\mu+\varepsilon+p)}. \tag{69}$$

The responsiveness of $\mathscr{R}_0$ may be investigated by taking into account the partial derivatives of reproductive number for the pertinent parameters.

$$\frac{\partial\mathscr{R}_0}{\partial\beta} = \frac{(\mu(1-q)+\varepsilon)}{(\mu+\gamma+\alpha)(\mu+\varepsilon+p)} > 0,$$

$$\frac{\partial\mathscr{R}_0}{\partial\mu} = \frac{(\mu+\gamma+\alpha)(\mu+\varepsilon+p)\beta(1-q) - \beta(\mu(1-q)+\varepsilon)\{2\mu+p+\varepsilon+\alpha+\gamma\}}{(\mu+\gamma+\alpha)^2(\mu+\varepsilon+p)^2} < 0,$$

$$\frac{\partial\mathscr{R}_0}{\partial q} = \frac{-\beta\mu}{(\mu+\gamma+\alpha)(\mu+\varepsilon+p)} < 0,$$

$$\frac{\partial\mathscr{R}_0}{\partial\varepsilon} = \frac{(\mu+\varepsilon+p)\beta - \beta(\mu(1-q)+\varepsilon)}{(\mu+\gamma+\alpha)(\mu+\varepsilon+p)^2} > 0,$$

$$\frac{\partial \mathscr{R}_0}{\partial \gamma} = -\frac{\beta(\mu(1-q)+\varepsilon)}{(\mu+\gamma+\alpha)^2(\mu+\varepsilon+p)} < 0,$$
$$\frac{\partial \mathscr{R}_0}{\partial \alpha} = -\frac{\beta(\mu(1-q)+\varepsilon)}{(\mu+\gamma+\alpha)^2(\mu+\varepsilon+p)} < 0,$$
$$\frac{\partial \mathscr{R}_0}{\partial p} = -\frac{\beta(\mu(1-q)+\varepsilon)}{(\mu+\gamma+\alpha)(\mu+\varepsilon+p)^2} < 0,$$

Clearly, $\mathscr{R}_0$ is quite sensitive to changes in the parameter. β and ε are expanding whereas μ, q, γ, α and p are decreasing in this study paper.

5.4 Uniqueness and Existence of the System

In this section, we have

Theorem 3. *Assume the existence of positive constants, λ_i, $\overline{\lambda}_i$ such that*

$$i. \qquad |H_i(x_i,t) - H_i(x_i^{'},t)| \leq \lambda_i |x_i - x_i^{'}| \qquad \forall i \in \{1,2,3\} \tag{70}$$

$$ii. \qquad |H_i(x_i,t)|^2 \leq \overline{\lambda_i}(1+|x_i|) \qquad \forall (x,t) \in R^3 \times [0,T] \tag{71}$$

Proof. We now recall our model

$$\begin{cases} {}_0^{CF}D_t^{\alpha} S(t) = (1-q)\Lambda - \frac{\beta SI}{N} - (\mu+p)S + \gamma I + \varepsilon V = H_1(t,S,I,V), \\ {}_0^{CF}D_t^{\alpha} I(t) = \frac{\beta SI}{N} - (\mu+\gamma+\alpha)I = H_2(t,S,I,V), \\ {}_0^{CF}D_t^{\alpha} V(t) = q\Lambda + pS - (\mu+\varepsilon)V = H_3(t,S,I,V). \end{cases} \tag{72}$$

We start with the function $H_1(t,S,I,V)$. Then, we will show that

$$\left|H_1(S^1,t) - H_1(S^2,t)\right|^2 \leq \lambda_1 \left|S^1 - S^2\right|^2. \tag{73}$$

Then, we write

$$\left|H_1(S^1,t) - H_1(S^2,t)\right|^2 = \left|-\frac{\beta I(S^1-S^2)}{N} - (\mu+p)(S^1-S^2)\right|^2, \tag{74}$$

$$\left|H_1(S^1,t) - H_1(S^2,t)\right|^2 = \left|-\left\{\frac{\beta I}{N} + \mu + p\right\}(S^1-S^2)\right|^2,$$

$$\left|H_1(S^1,t) - H_1(S^2,t)\right|^2 = \left|\left\{\frac{\beta I}{N} + \mu + p\right\}(S^1-S^2)\right|^2,$$

$$\left|H_1(S^1,t) - H_1(S^2,t)\right|^2 \leq \left\{2\frac{\beta^2|I|^2}{N^2} + 2(\mu+p)^2\right\}\left|(S^1-S^2)\right|^2,$$

$$\left|H_1(S^1,t) - H_1(S^2,t)\right|^2 \leq \left\{2\frac{\beta^2 \sup_{0\leq t\leq T}|I|^2}{N^2} + 2(\mu+p)^2\right\}\left|(S^1-S^2)\right|^2,$$

$$\left|H_1(S^1,t) - H_1(S^2,t)\right|^2 \leq \left\{2\frac{\beta^2|I|_{\infty}^2}{N^2} + 2(\mu+p)^2\right\}\left|(S^1-S^2)\right|^2,$$

$$\left|H_1(S^1,t) - H_1(S^2,t)\right|^2 \leq \lambda_1 \left|(S^1-S^2)\right|^2,$$

where

$$\lambda_1 = \left\{2\frac{\beta^2|I|_{\infty}^2}{N^2} + 2(\mu+p)^2\right\}.$$

$$\left|H_2(I^1,t) - H_2(I^2,t)\right|^2 = \left|-\frac{\beta S(I^1-I^2)}{N} - (\mu+\gamma+\alpha)(I^1-I^2)\right|^2, \tag{75}$$

$$\left|H_2(I^1,t)-H_2(I^2,t)\right|^2=\left|-\left\{\frac{\beta S}{N}+(\mu+\gamma+\alpha)\right\}(I^1-I^2)\right|^2,$$

$$\left|H_2(I^1,t)-H_2(I^2,t)\right|^2=\left|\left\{\frac{\beta S}{N}+(\mu+\gamma+\alpha)\right\}(I^1-I^2)\right|^2,$$

$$\left|H_2(I^1,t)-H_2(I^2,t)\right|^2\leq\left\{\frac{2\beta^2|S|^2}{N^2}+2(\mu+\gamma+\alpha)^2\right\}\left|(I^1-I^2)\right|^2,$$

$$\left|H_2(I^1,t)-H_2(I^2,t)\right|^2\leq\left\{\frac{2\beta^2\sup_{0\leq t\leq T}|S|^2}{N^2}+2(\mu+\gamma+\alpha)^2\right\}\left|(I^1-I^2)\right|^2,$$

$$\left|H_2(I^1,t)-H_2(I^2,t)\right|^2\leq\left\{\frac{2\beta^2|S|_\infty^2}{N^2}+2(\mu+\gamma+\alpha)^2\right\}\left|(I^1-I^2)\right|^2,$$

where

$$\lambda_2=\left\{\frac{2\beta^2|S|_\infty^2}{N^2}+2(\mu+\gamma+\alpha)^2\right\}.$$

$$\left|H_3(V^1,t)-H_3(V^2,t)\right|^2=\left|-(\mu+\varepsilon)(V^1-V^2)\right|^2,\tag{76}$$

$$\left|H_3(V^1,t)-H_3(V^2,t)\right|^2=\left|(\mu+\varepsilon)(V^1-V^2)\right|^2,$$

$$\left|H_3(V^1,t)-H_3(V^2,t)\right|^2\leq(\mu+\varepsilon)^2\left|(V^1-V^2)\right|^2,$$

$$\left|H_3(V^1,t)-H_3(V^2,t)\right|^2\leq\lambda_3\left|(V^1-V^2)\right|^2,$$

where

$$\lambda_3=\left\{(\mu+\varepsilon)^2\right\}.$$

We verified each function's initial condition twice. The second criterion of our model has now been verified.

$$|H_1(S,t)|^2=\left|(1-q)\Lambda-\frac{\beta SI}{N}-(\mu+p)S+\gamma I+\varepsilon V\right|^2,\tag{77}$$

$$|H_1(S,t)|^2=\left|(1-q)\Lambda+\gamma I+\varepsilon V-\left\{\frac{\beta I}{N}+(\mu+p)\right\}S\right|^2,$$

$$|H_1(S,t)|^2\leq 5\left\{(1-q)^2\Lambda^2+\gamma^2|I|+\varepsilon^2|V|+\left\{\frac{\beta|I|}{N}+(\mu+p)\right\}^2|S|^2\right\},$$

$$|H_1(S,t)|^2\leq 5\left\{(1-q)^2\Lambda^2+\gamma^2\sup_{0\leq t\leq T}|I|+\varepsilon^2\sup_{0\leq t\leq T}|V|+\left\{\frac{\beta\sup_{0\leq t\leq T}|I|}{N}+(\mu+p)\right\}^2|S|^2\right\},$$

$$|H_1(S,t)|^2\leq 5\left\{(1-q)^2\Lambda^2+\gamma^2|I|_\infty+\varepsilon^2|V|_\infty+\left\{\frac{\beta|I|_\infty}{N}+(\mu+p)\right\}^2|S|^2\right\},$$

$$|H_1(S,t)|^2\leq 5\left\{(1-q)^2\Lambda^2+\gamma^2|I|_\infty+\varepsilon^2|V|_\infty\right\}\left\{1+\frac{\left\{\frac{\beta|I|_\infty}{N}+(\mu+p)\right\}^2|S|^2}{5\left\{(1-q)^2\Lambda^2+\gamma^2|I|_\infty+\varepsilon^2|V|_\infty\right\}}\right\},$$

$$|H_1(S_1,t)|^2\leq\overline{\lambda}_1\left(1+|S|^2\right),$$

under the condition $\left[\frac{\left\{\frac{\beta|I|_\infty}{N}+(\mu+p)\right\}^2|S|^2}{5\left\{(1-q)^2\Lambda^2+\gamma^2|I|_\infty+\varepsilon^2|V|_\infty\right\}}\right]<1.$

$$|H_2(I,t)|^2=\left|\frac{\beta SI}{N}-(\mu+\gamma+\alpha)I\right|^2,\tag{78}$$

$$|H_2(I,t)|^2 = \left|\left\{\frac{\beta S}{N} - (\mu+\gamma+\alpha)\right\} I\right|^2,$$

$$|H_2(I,t)|^2 \leq 2\left\{\frac{\beta^2|S|^2}{N^2} + 2(\mu+\gamma+\alpha)^2\right\}|I|^2,$$

$$|H_2(I,t)|^2 \leq 2\left\{\frac{\beta^2 \sup_{0\leq t\leq T}|S|^2}{N^2} + 2(\mu+\gamma+\alpha)^2\right\}|I|^2,$$

$$|H_2(I,t)|^2 \leq 2\left\{\frac{\beta^2|S|_\infty^2}{N^2} + 2(\mu+\gamma+\alpha)^2\right\}|I|^2,$$

$$|H_2(I,t)|^2 \leq 2\left\{\frac{\beta^2|S|_\infty^2}{N^2} + 2(\mu+\gamma+\alpha)^2\right\}\left\{1+|I|^2\right\},$$

$$|H_2(I,t)|^2 \leq \overline{\lambda}_2\left(1+|I|^2\right).$$

$$|H_3(V,t)|^2 = |q\Lambda + pS - (\mu+\varepsilon)V|^2, \tag{79}$$

$$|H_3(V,t)|^2 \leq 3q^2\Lambda^2 + 3p^2|S|^2 + 3(\mu+\varepsilon)^2|V|^2,$$

$$|H_3(V,t)|^2 \leq 3q^2\Lambda^2 + 3p^2 \sup_{0\leq t\leq T}|S|^2 + 3(\mu+\varepsilon)^2|V|^2,$$

$$|H_3(V,t)|^2 \leq 3q^2\Lambda^2 + 3p^2|S|_\infty^2 + 3(\mu+\varepsilon)^2|V|^2,$$

$$|H_3(V,t)|^2 \leq 3\left\{q^2\Lambda^2 + 3p^2|S|_\infty^2\right\}\left\{1 + \frac{(\mu+\varepsilon)^2|V|^2}{\{q^2\Lambda^2+3p^2|S|_\infty^2\}}\right\},$$

$$|H_3(V,t)|^2 \leq \overline{\lambda}_3\left(1+|V|^2\right),$$

under the condition $\left\{\frac{(\mu+\varepsilon)^2|V|^2}{\{q^2\Lambda^2+3p^2|S|_\infty^2\}}\right\} < 1$.

The solution to the system we have ultimately arises and is unique in light of the conditions at hand.

$$Max\left\{\begin{array}{l}\left[\frac{\left\{\frac{\beta|I|_\infty}{N}+(\mu+p)\right\}^2|S|^2}{5\left\{(1-q)^2\Lambda^2+\gamma^2|I|_\infty+\varepsilon^2|V|_\infty\right\}}\right], \\ \left\{\frac{(\mu+\varepsilon)^2|V|^2}{\{q^2\Lambda^2+3p^2|S|_\infty^2\}}\right\}.\end{array}\right. \quad < 1 \tag{80}$$

5.5 Local Asymptotical Stability

Letting $F = \frac{\beta SI}{N}$, the Jacobian matrix of the model (37) at $E^\star$ has the following form

$$J^\star = \begin{bmatrix} b_1 - (\mu+\gamma+\alpha) & b_2 & b_3 \\ -b_1+\gamma & -b_2-(\mu+p) & -b_3+\varepsilon \\ 0 & p & -(\mu+\varepsilon) \end{bmatrix} \tag{81}$$

in which

$$b_1 = \frac{\partial F}{\partial I}\Big|_{E^\star} = \frac{\beta S^\star(N^\star - I^\star)}{N^{\star 2}}, \tag{82}$$

$$b_2 = \frac{\partial F}{\partial S}\Big|_{E^\star} = \frac{\beta S^\star(N^\star - I^\star)}{N^{\star 2}}, \tag{83}$$

$$b_3 = \frac{\partial F}{\partial V}\Big|_{E^\star} = -\frac{\beta S^\star I^\star}{N^{\star 2}}. \tag{84}$$

The characteristic equation of matrix $J^\star$ is

$$\Upsilon(\lambda) = b_3 + b_2\lambda + b_1\lambda^2 + \lambda^3, \tag{85}$$

where

$$a_1 = -trs(J^\star),$$

$$a_1 = -b_1 + b_2 + (\mu+\gamma+\alpha) + (2\mu+p+\varepsilon). \tag{86}$$

$$a_2 = -\frac{1}{2}(trs(J^{\star 2}) - trs^2 J^\star),$$

$$a_2 = -b_1 + b_2 + (\mu+\gamma+\alpha) + (2\mu+p+\varepsilon),$$

$$= -b_1(2\mu+p+\varepsilon) + b_2(2\mu+p+\varepsilon) + b_3 p + \mu(\mu+p+\varepsilon) + (\mu+\gamma+\alpha). \tag{87}$$

$$a_3 = -(detJ^\star),$$

$$a_3 = -b_1\mu(\mu+p+\varepsilon) + b_2(\mu+\alpha)(\mu+\varepsilon) + b_3 p(\mu+\alpha) + \mu(\mu+\gamma+\alpha)(\mu+p+\varepsilon). \tag{88}$$

We have

$$b_1 = (\mu+\gamma+\alpha)\left\{1 - \frac{\mu(\mathscr{R}_0-1)}{\mu\widehat{\mathscr{R}}_0 + \alpha(\widehat{\mathscr{R}}_0 - \mathscr{R}_0)}\right\}. \tag{89}$$

$$b_2 = \mu(\beta - (\mu+\gamma+\alpha))\left\{\frac{(\mathscr{R}_0-1)}{\mu\widehat{\mathscr{R}}_0 + \alpha(\widehat{\mathscr{R}}_0 - \mathscr{R}_0)}\right\}. \tag{90}$$

$$b_3 = -\mu(\mu+\gamma+\alpha)\left\{\frac{(\mathscr{R}_0-1)}{\mu\widehat{\mathscr{R}}_0 + \alpha(\widehat{\mathscr{R}}_0 - \mathscr{R}_0)}\right\}. \tag{91}$$

Obviously $b_3 < 0$ and $b_1 = (\mu+\gamma+\alpha)\left\{\frac{(\mu+\alpha)(\widehat{\mathscr{R}}_0-\mathscr{R}_0)+\mu}{\mu\widehat{\mathscr{R}}_0+\alpha(\widehat{\mathscr{R}}_0-\mathscr{R}_0)}\right\} > 0$.

Moreover, notice that the equilibrium $E^\star$ exists if $\mathscr{R}_0 > 1$ and this implies

$$\beta > \beta\left\{\frac{\mu(1-q)+\varepsilon}{\mu+p+\varepsilon}\right\} > (\mu+\gamma+\alpha), \tag{92}$$

and thus, $b_2 > 0$.

Using equation (92), we obtain Now

$$-b_1 + b_2 = -(\mu+\gamma+\alpha) + \mu\beta\left\{\frac{\mathscr{R}_0-1}{\mu\widehat{\mathscr{R}}_0 + \alpha(\widehat{\mathscr{R}}_0 - \mathscr{R}_0)}\right\}, \tag{93}$$

thus

$$a_1 = \mu\beta\left\{\frac{\mathscr{R}_0-1}{\mu\widehat{\mathscr{R}}_0 + \alpha(\widehat{\mathscr{R}}_0 - \mathscr{R}_0)}\right\} + (2\mu+p+\varepsilon) > 0. \tag{94}$$

We can see that

$$-b_1(2\mu+p+\varepsilon) + b_3 p + (\mu+\gamma+\alpha)(2\mu+p+\varepsilon) = (\mu+\gamma+\alpha)(2\mu+\varepsilon)\left\{\frac{\mathscr{R}_0-1}{\mu\widehat{\mathscr{R}}_0 + \alpha(\widehat{\mathscr{R}}_0 - \mathscr{R}_0)}\right\}, \tag{95}$$

and therefore,

$$a_2 = (\mu+\gamma+\alpha)(2\mu+\varepsilon)\left\{\frac{\mathscr{R}_0-1}{\mu\widehat{\mathscr{R}}_0 + \alpha(\widehat{\mathscr{R}}_0 - \mathscr{R}_0)}\right\} + b_2(2\mu+\alpha+\varepsilon) + \mu(\mu+p+\varepsilon) > 0. \tag{96}$$

Now we have

$$a_3 = \mu(\mu+p+\varepsilon)(\mu+\gamma+\alpha)\left\{\frac{\mu(\mathscr{R}_0-1)}{\mu\widehat{\mathscr{R}}_0+\alpha(\widehat{\mathscr{R}}_0-\mathscr{R}_0)}\right\}+(\beta(\mu+\varepsilon) - (\mu+p+\varepsilon)(\mu+\gamma+\alpha))\mu(\mu+\alpha)\left\{\frac{\mathscr{R}_0-1}{\mu\widehat{\mathscr{R}}_0+\alpha(\widehat{\mathscr{R}}_0-\mathscr{R}_0)}\right\} + \mu(\mu+p+\varepsilon)(\mu+\gamma+\alpha). \tag{97}$$

Besides, $\widehat{\mathscr{R}}_0 > \mathscr{R}_0$ and $\mathscr{R}_0 > 1$ implies $\beta(\mu+\varepsilon) > (\mu+p+\varepsilon)(\mu+\gamma+\alpha)$.

Therefore,

$$a_3 > \mu(\mu+p+\varepsilon)(\mu+\gamma+\alpha)\left\{1+\frac{\mu(\mathscr{R}_0-1)}{\mu\widehat{\mathscr{R}}_0+\alpha(\widehat{\mathscr{R}}_0-\mathscr{R}_0)}\right\} > 0. \tag{98}$$

Now we have

$$a_1a_2-a_3 = (\mu+\varepsilon)(a_2-b_2(\mu+\alpha))+(\mu+\gamma+\alpha)(a_2-\mu(\mu+p+\varepsilon))+(-b_1+b_2+\mu+p)a_2 + b_1\mu(\mu+p+\varepsilon)-b_3p(\mu+\alpha), \tag{99}$$

$$= (\mu+\varepsilon)(a_2-b_2(\mu+\alpha))+((\mu+\gamma+\alpha)-b_1)(a_2-\mu(\mu+p+\varepsilon))+(b_2+\mu+p)a_2-b_3\mu(\mu+\alpha).$$

We see that $b_1 = (\mu+\gamma+\alpha)\left\{1-\frac{\mu(\mathscr{R}_0-1)}{\mu\widehat{\mathscr{R}}_0+\alpha(\widehat{\mathscr{R}}_0-\mathscr{R}_0)}\right\} < (\mu+\gamma+\alpha)$,and as a result

$$a_1a_2-a_3 > (\mu+\varepsilon)(a_2-b_2(\mu+\alpha))+(b_2+\mu+p)a_2-b_3p(\mu+\alpha) > 0. \tag{100}$$

In preceding relations, we got $a_1 > 0, a_2 > 0, a_3 > 0$ and $a_1a_2-a_3 > 0$. Its satisfied Routh Hurwitz criterion, hence proved.

5.6 Global Stability Analysis of the Proposed Model

We first investigate the stability characteristics of the infectious epidemic model.

5.7 Lyapunov for Endemic Case of the Infectious Model

All independent variables in the model were established using the endemic Lyapunov function in our case, the harmful equilibrium is $\{S,I,V\}, L < 0, E^\star$.

5.7.1 First Derivative of Lyapunov

Theorem 4. *The Lyapunov function, $\{S,I,V\}$, $L < 0$ are endemic functions. The endemic equilibrium is E^*. The suggested model's endemic equilibrium points $E^\star$ are globally asymptotically stable when the reproductive number $\mathscr{R}_0 > 1$.*

Proof. The Lyapunov function is used to establish the theorem in the following way

$$\mathbb{L}(S^\star,I^\star,V^\star) = \left(S-S^\star-S^\star\log\frac{S^\star}{S}\right)+\left(I-I^\star-I^\star\log\frac{I^\star}{I}\right)+\left(V-V^\star-V^\star\log\frac{V^\star}{V}\right). \tag{101}$$

As a result, when we use the derivative with respect to t, we get the following.

$${}_0^{CF}D_t^\alpha\mathbb{L} \le \left(\frac{S-S^\star}{S}\right)\dot{S}+\left(\frac{I-I^\star}{I}\right)\dot{I}+\left(\frac{V-V^\star}{V}\right)\dot{V}. \tag{102}$$

The following is how their derivative values may now be written

$$\begin{aligned} {}_0^{CF}D_t^{\alpha}\mathbb{L} \leq & \left(\frac{S-S^{\star}}{S}\right)\left((1-q)\Lambda-\frac{\beta SI}{N}-(\mu+p)S+\gamma I+\varepsilon V\right) \\ & +\left(\frac{I-I^{\star}}{I}\right)\left(\frac{\beta SI}{N}-(\mu+\gamma+\alpha)I\right) \\ & +\left(\frac{V-V^{\star}}{V}\right)\left(q\Lambda+pS-(\mu+\varepsilon)V\right). \end{aligned} \tag{103}$$

substituting values $S=S-S^{\star}$, $I=I-I^{\star}$ and $V=V-V^{\star}$ leads to

$$\begin{aligned} {}_0^{CF}D_t^{\alpha}\mathbb{L} \leq & \left(\frac{S-S^{\star}}{S}\right)\left((1-q)\Lambda-\frac{\beta(S-S^{\star})(I-I^{\star})}{N}-(\mu+p)(S-S^{\star})+\gamma(I-I^{\star})+\varepsilon(V-V^{\star})\right) \\ & +\left(\frac{I-I^{\star}}{I}\right)\left(\frac{\beta(S-S^{\star})(I-I^{\star})}{N}-(\mu+\gamma+\alpha)(I-I^{\star})\right) \\ & +\left(\frac{V-V^{\star}}{V}\right)\left(q\Lambda+p(S-S^{\star})-(\mu+\varepsilon)(V-V^{\star})\right). \end{aligned} \tag{104}$$

The above can be organized as follows

$$\begin{aligned} {}_0^{CF}D_t^{\alpha}\mathbb{L} \leq & \Lambda-\frac{\Lambda S^{\star}}{S}-q\Lambda+\frac{q\Lambda S^{\star}}{S}-\frac{\beta I(S-S^{\star})^2}{SN}+\frac{\beta I^{\star}(S-S^{\star})^2}{SN}-\frac{(\mu+p)(S-S^{\star})^2}{S}+\gamma I-\gamma I^{\star} \\ & -\frac{\gamma IS^{\star}}{S}+\frac{\gamma I^{\star}S^{\star}}{S}+\varepsilon V-\varepsilon V^{\star}-\frac{\varepsilon VS^{\star}}{S}+\frac{\varepsilon V^{\star}S^{\star}}{S}+\frac{\beta S(I-I^{\star})^2}{NI}-\frac{\beta S^{\star}(I-I^{\star})^2}{NI} \\ & -\frac{(\mu+\gamma+\alpha)(I-I^{\star})^2}{I}+q\Lambda+pS-pS^{\star}-\frac{q\Lambda V^{\star}}{V}-\frac{pSV^{\star}}{V}+\frac{pS^{\star}V^{\star}}{V}-\frac{(\mu+\varepsilon)(V-V^{\star})^2}{V}. \end{aligned} \tag{105}$$

For clarity, we may rewrite the above equivalency as follows

$${}_0^{CF}D_t^{\alpha}\mathbb{L} \leq \Theta-\Theta^{\star}, \tag{106}$$

where

$$\Theta=\Lambda+\frac{q\Lambda S^{\star}}{S}+\frac{\beta I^{\star}(S-S^{\star})^2}{SN}+\gamma I+\frac{\gamma I^{\star}S^{\star}}{S}+\varepsilon V+\frac{\varepsilon V^{\star}S^{\star}}{S}+\frac{\beta S(I-I^{\star})^2}{NI}+q\Lambda+pS+\frac{pS^{\star}V^{\star}}{V}, \tag{107}$$

and

$$\begin{aligned} \Theta^{\star}= & \frac{\Lambda S^{\star}}{S}+q\Lambda+\frac{\beta I(S-S^{\star})^2}{SN}+\frac{(\mu+p)(S-S^{\star})^2}{S}+\gamma I^{\star}+\frac{\gamma IS^{\star}}{S}+\varepsilon V^{\star}+\frac{\varepsilon VS^{\star}}{S}+\frac{\beta S^{\star}(I-I^{\star})^2}{NI} \\ & +\frac{(\mu+\gamma+\alpha)(I-I^{\star})^2}{I}+pS^{\star}+\frac{q\Lambda V^{\star}}{V}+\frac{pSV^{\star}}{V}+\frac{(\mu+\varepsilon)(V-V^{\star})^2}{V}. \end{aligned} \tag{108}$$

It is achieved that if $\Theta<\Theta^{\star}$, this yields ${}_0^{CF}D_t^{\alpha}\mathbb{L}<0$, however when $S=S^{\star}$, $I=I^{\star}$ and $V=V^{\star}$

$$0=\Theta-\Theta^{\star} \qquad \Rightarrow \qquad {}_0^{CF}D_t^{\alpha}\mathbb{L}=0. \tag{109}$$

The recommended model has the largest compact invariant set, as can be shown.

$$\left\{(S^{\star},I^{\star},V^{\star})\in\Gamma;{}_0^{CF}D_t^{\alpha}\mathbb{L}=0\right\}. \tag{110}$$

The model under examination has an endemic equilibrium called $E^{\star}$. The Lasalles invariance principle states that if $\Theta<\Theta^{\star}$ is globally asymptotically stable in Γ, then $E^{\star}$ is also worldwide asymptotically stable in Γ.

5.7.2 Second Derivative of Lyapunov

The second derivative, in our opinion, will add more details.

$$ {}_0^{CF}D_t^{\alpha}({}_0^{CF}D_t^{\alpha}\mathbb{L}) = {}_0^{CF}D_t^{\alpha}\dot{\mathbb{L}} = {}_0^{CF}D_t^{\alpha}\left\{\left(1-\frac{S^{\star}}{S}\right){}_0^{CF}D_t^{\alpha}S+\left(1-\frac{I^{\star}}{I}\right){}_0^{CF}D_t^{\alpha}I+\left(1-\frac{V^{\star}}{V}\right){}_0^{CF}D_t^{\alpha}V\right\}. \tag{111} $$

$$ \begin{aligned} &= \left(\frac{{}_0^{CF}D_t^{\alpha}S}{S}\right)^2 S^* + \left(\frac{{}_0^{CF}D_t^{\alpha}I}{I}\right)^2 I^* + \left(\frac{{}_0^{CF}D_t^{\alpha}V}{V}\right)^2 V^* \\ &+ \left(1-\frac{S^*}{S}\right){}_0^{CF}D_t^{\alpha}\dot{S} + \left(1-\frac{I^*}{I}\right){}_0^{CF}D_t^{\alpha}\dot{I} + \left(1-\frac{V^*}{V}\right){}_0^{CF}D_t^{\alpha}\dot{V}, \end{aligned} \tag{112} $$

Then we have

$$ \begin{aligned} &= \left(\frac{{}_0^{CF}D_t^{\alpha}S}{S}\right)^2 S^* + \left(\frac{{}_0^{CF}D_t^{\alpha}I}{I}\right)^2 I^* + \left(\frac{{}_0^{CF}D_t^{\alpha}V}{V}\right)^2 V^* \\ &+ \left(1-\frac{S^*}{S}\right)\left(-\frac{\beta S[{}_0^{CF}D_t^{\alpha}I]+\beta[{}_0^{CF}D_t^{\alpha}S]I}{N} - (\mu+p)[{}_0^{CF}D_t^{\alpha}S] + \gamma[{}_0^{CF}D_t^{\alpha}I] + \varepsilon[{}_0^{CF}D_t^{\alpha}V]\right) \\ &+ \left(1-\frac{I^*}{I}\right)\left(\frac{\beta S[{}_0^{CF}D_t^{\alpha}I]+\beta[{}_0^{CF}D_t^{\alpha}S]I}{N} - (\mu+\gamma+\alpha)[{}_0^{CF}D_t^{\alpha}I]\right) \\ &+ \left(1-\frac{I^*}{V}\right)\left(p[{}_0^{CF}D_t^{\alpha}S] - (\mu+\varepsilon)[{}_0^{CF}D_t^{\alpha}V]\right) \end{aligned} \tag{113} $$

$$ \begin{aligned} =&\dot{\Pi}(S,I,V) + \left(1-\frac{S^*}{S}\right)\left(-\frac{\beta S[{}_0^{CF}D_t^{\alpha}I]+\beta[{}_0^{CF}D_t^{\alpha}S]I}{N} - (\mu+p)[{}_0^{CF}D_t^{\alpha}S] + \gamma[{}_0^{CF}D_t^{\alpha}I] + \varepsilon[{}_0^{CF}D_t^{\alpha}V]\right) \\ &+ \left(1-\frac{I^*}{I}\right)\left(\frac{\beta S[{}_0^{CF}D_t^{\alpha}I]+\beta[{}_0^{CF}D_t^{\alpha}S]I}{N} - (\mu+\gamma+\alpha)[{}_0^{CF}D_t^{\alpha}I]\right) + \left(1-\frac{I^*}{V}\right)\left(p[{}_0^{CF}D_t^{\alpha}S] - (\mu+\varepsilon)[{}_0^{CF}D_t^{\alpha}V]\right). \end{aligned} \tag{114} $$

Now replacing $\dot{S}$, $\dot{I}$ and $\dot{V}$ with their respective formula and then putting together positive and negative factors, we have

$$ {}_0^{CF}D_t^{\alpha}\dot{\mathbb{L}} = \Theta_1 - \Theta_2. \tag{115} $$

Then we have

$$ \begin{array}{llll} If & \Theta_1 > \Theta_2 & then & {}_0^{CF}D_t^{\alpha}\dot{\mathbb{L}} > 0, \\ If & \Theta_1 < \Theta_2 & then & {}_0^{CF}D_t^{\alpha}\dot{\mathbb{L}} < 0, \\ If & \Theta_1 = \Theta_2 & then & {}_0^{CF}D_t^{\alpha}\dot{\mathbb{L}} = 0. \end{array} \tag{116} $$

Following that, the second-order sign's significance is explained.

5.8 Numerical Scheme with Different Kernel

In this section, we used different kernel such as exponential decay, power law and Mittag Leffler kernels with fractal fractional operator for numerical solution.

First, consider exponential decay kernel for system

$$ \begin{cases} {}^{FFE}\mathbb{D}_{0,t}^{\alpha,\kappa_1}S(t) = (1-q)\Lambda - \frac{\beta SI}{N} - (\mu+p)S + \gamma I + \varepsilon V, \\ {}^{FFE}\mathbb{D}_{0,t}^{\alpha,\kappa_1}I(t) = \frac{\beta SI}{N} - (\mu+\gamma+\alpha)I, \\ {}^{FFE}\mathbb{D}_{0,t}^{\alpha,\kappa_1}V(t) = q\Lambda + pS - (\mu+\varepsilon)V. \end{cases} \tag{117} $$

For simplicity, we write above equation as follows

$$ \begin{cases} {}^{FFE}\mathbb{D}_{0,t}^{\alpha,\kappa_1}S(t) = \mathscr{G}_1(t,S,I,V), \\ {}^{FFE}\mathbb{D}_{0,t}^{\alpha,\kappa_1}I(t) = \mathscr{G}_2(t,S,I,V), \\ {}^{FFE}\mathbb{D}_{0,t}^{\alpha,\kappa_1}V(t) = \mathscr{G}_3(t,S,I,V). \end{cases} \tag{118} $$

Where

$$\begin{cases} \mathscr{G}_1(t,S,I,V) = (1-q)\Lambda - \frac{\beta SI}{N} - (\mu+p)S + \gamma I + \varepsilon V, \\ \mathscr{G}_2(t,S,I,V) = \frac{\beta SI}{N} - (\mu+\gamma+\alpha)I, \\ \mathscr{G}_3(t,S,I,V) = q\Lambda + pS - (\mu+\varepsilon)V. \end{cases} \tag{119}$$

The subsequent results are obtained by using a fractal fractional integral with an exponential kernel:

$$\begin{aligned} S(t_{n+1}) = S(t_n) &+ \frac{1-\alpha}{\mathscr{M}(\alpha)}\left[t_n^{1-\kappa_1}\mathscr{G}_1(t_n,S(t_n),I(t_n),V(t_n)) - t_{n-1}^{1-\kappa_1}\mathscr{G}_1(t_{n-1},S(t_{n-1}),I(t_{n-1}),V(t_{n-1}))\right] \\ &+ \frac{\alpha}{\mathscr{M}(\alpha)}\int_{t_n}^{t_{n+1}}\mathscr{G}_1(t,S,I,V)\vartheta^{1-\kappa_1}d\vartheta, \end{aligned} \tag{120}$$

$$\begin{aligned} I(t_{n+1}) = I(t_n) &+ \frac{1-\alpha}{\mathscr{M}(\alpha)}\left[t_n^{1-\kappa_1}\mathscr{G}_2(t_n,S(t_n),I(t_n),V(t_n)) - t_{n-1}^{1-\kappa_1}\mathscr{G}_2(t_{n-1},S(t_{n-1}),I(t_{n-1}),V(t_{n-1}))\right] \\ &+ \frac{\alpha}{\mathscr{M}(\alpha)}\int_{t_n}^{t_{n+1}}\mathscr{G}_2(t,S,I,V)\vartheta^{1-\kappa_1}d\vartheta, \end{aligned} \tag{121}$$

$$\begin{aligned} V(t_{n+1}) = V(t_n) &+ \frac{1-\alpha}{\mathscr{M}(\alpha)}\left[t_n^{1-\kappa_1}\mathscr{G}_3(t_n,S(t_n),I(t_n),V(t_n)) - t_{n-1}^{1-\kappa_1}\mathscr{G}_3(t_{n-1},S(t_{n-1}),I(t_{n-1}),V(t_{n-1}))\right] \\ &+ \frac{\alpha}{\mathscr{M}(\alpha)}\int_{t_n}^{t_{n+1}}\mathscr{G}_3(t,S,I,V)\vartheta^{1-\kappa_1}d\vartheta. \end{aligned} \tag{122}$$

For this particular model, we might employ the subsequent technique.

$$\begin{aligned} S(t_{n+1}) = S_n &+ \frac{1-\alpha}{\mathscr{M}(\alpha)}\left[t_n^{1-\kappa_1}\mathscr{G}_1(t_n,S(t_n),I(t_n),V(t_n)) - t_{n-1}^{1-\kappa_1}\mathscr{G}_1(t_{n-1},S(t_{n-1}),I(t_{n-1}),V(t_{n-1}))\right] \\ &+ \frac{\alpha}{\mathscr{M}(\alpha)}\left[\frac{23t_n^{1-\kappa_1}\mathscr{G}_1(t_n,S(t_n),I(t_n),V(t_n))\Delta t}{12} - \frac{4t_{n-1}^{1-\kappa_1}\mathscr{G}_1(t_{n-1},S(t_{n-1}),I(t_{n-1}),V(t_{n-1}))\Delta t}{3}\right. \\ &\left. + \frac{5t_{n-2}^{1-\kappa_1}\mathscr{G}_1(t_{n-2},S(t_{n-2}),I(t_{n-2}),V(t_{n-2}))\Delta t}{12}\right], \end{aligned} \tag{123}$$

$$\begin{aligned} I(t_{n+1}) = I_n &+ \frac{1-\alpha}{\mathscr{M}(\alpha)}\left[t_n^{1-\kappa_1}\mathscr{G}_2(t_n,S(t_n),I(t_n),V(t_n)) - t_{n-1}^{1-\kappa_1}\mathscr{G}_2(t_{n-1},S(t_{n-1}),I(t_{n-1}),V(t_{n-1}))\right] \\ &+ \frac{\alpha}{\mathscr{M}(\alpha)}\left[\frac{23t_n^{1-\kappa_1}\mathscr{G}_2(t_n,S(t_n),I(t_n),V(t_n))\Delta t}{12} - \frac{4t_{n-1}^{1-\kappa_1}\mathscr{G}_2(t_{n-1},S(t_{n-1}),I(t_{n-1}),V(t_{n-1}))\Delta t}{3}\right. \\ &\left. + \frac{5t_{n-2}^{1-\kappa_1}\mathscr{G}_2(t_{n-2},S(t_{n-2}),I(t_{n-2}),V(t_{n-2}))\Delta t}{12}\right], \end{aligned} \tag{124}$$

$$\begin{aligned} V(t_{n+1}) = V_n &+ \frac{1-\alpha}{\mathscr{M}(\alpha)}\left[t_n^{1-\kappa_1}\mathscr{G}_3(t_n,S(t_n),I(t_n),V(t_n)) - t_{n-1}^{1-\kappa_1}\mathscr{G}_3(t_{n-1},S(t_{n-1}),I(t_{n-1}),V(t_{n-1}))\right] \\ &+ \frac{\alpha}{\mathscr{M}(\alpha)}\left[\frac{23t_n^{1-\kappa_1}\mathscr{G}_3(t_n,S(t_n),I(t_n),V(t_n))\Delta t}{12} - \frac{4t_{n-1}^{1-\kappa_1}\mathscr{G}_3(t_{n-1},S(t_{n-1}),I(t_{n-1}),V(t_{n-1}))\Delta t}{3}\right. \\ &\left. + \frac{5t_{n-2}^{1-\kappa_1}\mathscr{G}_3(t_{n-2},S(t_{n-2}),I(t_{n-2}),V(t_{n-2}))\Delta t}{12}\right]. \end{aligned} \tag{125}$$

For Power Law kernel, we can have the following

$$S(t_{n+1}) = \frac{1}{\Gamma(\alpha)}\sum_{j=2}^{n}\int_{t_j}^{t_{j+1}}\mathscr{G}_1(\vartheta,S,I,V)\vartheta^{1-\kappa_1}(t_{n+1}-\vartheta)^{\alpha-1}d\vartheta, \tag{126}$$

$$I(t_{n+1}) = \frac{1}{\Gamma(\alpha)}\sum_{j=2}^{n}\int_{t_j}^{t_{j+1}}\mathscr{G}_2(\vartheta,S,I,V)\vartheta^{1-\kappa_1}(t_{n+1}-\vartheta)^{\alpha-1}d\vartheta, \tag{127}$$

$$V(t_{n+1}) = \frac{1}{\Gamma(\alpha)}\sum_{j=2}^{n}\int_{t_j}^{t_{j+1}}\mathscr{G}_3(\vartheta,S,I,V)\vartheta^{1-\kappa_1}(t_{n+1}-\vartheta)^{\alpha-1}d\vartheta. \tag{128}$$

A subsequent numerical pattern can be obtained.

$$\begin{aligned} S(t_{n+1}) &= \frac{(\Delta t)^{\alpha}}{\Gamma(\alpha+1)}\sum_{j=2}^{n} t_{j-2}^{1-\kappa_1}\mathscr{G}_1(t_{j-2},S_{j-2},I_{j-2},V_{j-2})\times \mathbf{W_1} \\ &+ \frac{(\Delta t)^{\alpha}}{\Gamma(\alpha+2)}\sum_{j=2}^{n}\left[t_{j-1}^{1-\kappa_1}\mathscr{G}_1(t_{j-1},S_{j-1},I_{j-1},V_{j-1}) - t_{j-2}^{1-\kappa_1}\mathscr{G}_1(t_{j-2},S_{j-2},I_{j-2},V_{j-2})\right]\times \mathbf{W_2} \\ &\sum_{j=2}^{n}\left[t_{j}^{1-\kappa_1}\mathscr{G}_1(t_{j},S_{j},I_{j},V_{j}) - 2t_{j-1}^{1-\kappa_1}\mathscr{G}_1(t_{j-1},S_{j-1},I_{j-1},V_{j-1}) - t_{j-2}^{1-\kappa_1}\mathscr{G}_1(t_{j-2},S_{j-2},I_{j-2},V_{j-2})\right]\times \mathbf{W_3}, \end{aligned} \tag{129}$$

$$\begin{aligned} I(t_{n+1}) &= \frac{(\Delta t)^{\alpha}}{\Gamma(\alpha+1)}\sum_{j=2}^{n} t_{j-2}^{1-\kappa_1}\mathscr{G}_2(t_{j-2},S_{j-2},I_{j-2},V_{j-2})\times \mathbf{W_1} \\ &+ \frac{(\Delta t)^{\alpha}}{\Gamma(\alpha+2)}\sum_{j=2}^{n}\left[t_{j-1}^{1-\kappa_1}\mathscr{G}_2(t_{j-1},S_{j-1},I_{j-1},V_{j-1}) - t_{j-2}^{1-\kappa_1}\mathscr{G}_2(t_{j-2},S_{j-2},I_{j-2},V_{j-2})\right]\times \mathbf{W_2} \\ &\sum_{j=2}^{n}\left[t_{j}^{1-\kappa_1}\mathscr{G}_2(t_{j},S_{j},I_{j},V_{j}) - 2t_{j-1}^{1-\kappa_1}\mathscr{G}_2(t_{j-1},S_{j-1},I_{j-1},V_{j-1}) - t_{j-2}^{1-\kappa_1}\mathscr{G}_2(t_{j-2},S_{j-2},I_{j-2},V_{j-2})\right]\times \mathbf{W_3}, \end{aligned} \tag{130}$$

$$\begin{aligned} V(t_{n+1}) &= \frac{(\Delta t)^{\alpha}}{\Gamma(\alpha+1)}\sum_{j=2}^{n} t_{j-2}^{1-\kappa_1}\mathscr{G}_3(t_{j-2},S_{j-2},I_{j-2},V_{j-2})\times \mathbf{W_1} \\ &+ \frac{(\Delta t)^{\alpha}}{\Gamma(\alpha+2)}\sum_{j=2}^{n}\left[t_{j-1}^{1-\kappa_1}\mathscr{G}_3(t_{j-1},S_{j-1},I_{j-1},V_{j-1}) - t_{j-2}^{1-\kappa_1}\mathscr{G}_3(t_{j-2},S_{j-2},I_{j-2},V_{j-2})\right]\times \mathbf{W_2} \\ &\sum_{j=2}^{n}\left[t_{j}^{1-\kappa_1}\mathscr{G}_3(t_{j},S_{j},I_{j},V_{j}) - 2t_{j-1}^{1-\kappa_1}\mathscr{G}_3(t_{j-1},S_{j-1},I_{j-1},V_{j-1}) - t_{j-2}^{1-\kappa_1}\mathscr{G}_3(t_{j-2},S_{j-2},I_{j-2},V_{j-2})\right]\times \mathbf{W_3}. \end{aligned} \tag{131}$$

Where

$$\mathbf{W_1} = \{(n-j+1)^{\alpha} - (n-j)^{\alpha}\}, \tag{132}$$

$$\mathbf{W_2} = \{(n-j+1)^{\alpha}(n-j+3+2\alpha) - (n-j)^{\alpha}(n-j+3+3\alpha)\} + \frac{(\Delta t)^{\alpha}}{2\Gamma(\alpha+3)}, \tag{133}$$

$$\begin{aligned} \mathbf{W_3} = \Big\{&(n-j+1)^{\alpha}\left\{2(n-j)^2 + (5\alpha+10)(n-j) + 6\alpha^2 + 18\alpha + 12\right\} \\ &- (n-j)^{\alpha}\left\{2(n-j)^2 + (3\alpha+10)(n-j) + 2\alpha^2 + 9\alpha + 12\right\}\Big\}. \end{aligned} \tag{134}$$

For Mittag- Leffler kernel, we can have the following

$$\begin{aligned} S(t_{n+1}) &= S_0 + \frac{1-\alpha}{\mathscr{AB}(\alpha)} t_n^{1-\kappa_1}\mathscr{G}_1(t_n,S_n,I_n,V_n) \\ &+ \frac{\alpha}{\Gamma(\alpha)\mathscr{AB}(\alpha)}\sum_{j=2}^{n}\int_{t_j}^{t_{j+1}} \mathscr{G}_1(\vartheta,S,I,V)\vartheta^{1-\kappa_1}(t_{n+1}-\vartheta)^{\alpha-1}d\vartheta, \end{aligned} \tag{135}$$

$$\begin{aligned} I(t_{n+1}) &= I_0 + \frac{1-\alpha}{\mathscr{AB}(\alpha)} t_n^{1-\kappa_1}\mathscr{G}_2(t_n,S_n,I_n,V_n) \\ &+ \frac{\alpha}{\Gamma(\alpha)\mathscr{AB}(\alpha)}\sum_{j=2}^{n}\int_{t_j}^{t_{j+1}} \mathscr{G}_2(\vartheta,S,I,V)\vartheta^{1-\kappa_1}(t_{n+1}-\vartheta)^{\alpha-1}d\vartheta, \end{aligned} \tag{136}$$

$$\begin{aligned} V(t_{n+1}) &= V_0 + \frac{1-\alpha}{\mathscr{AB}(\alpha)} t_n^{1-\kappa_1}\mathscr{G}_3(t_n,S_n,I_n,V_n) \\ &+ \frac{\alpha}{\Gamma(\alpha)\mathscr{AB}(\alpha)}\sum_{j=2}^{n}\int_{t_j}^{t_{j+1}} \mathscr{G}_3(\vartheta,S,I,V)\vartheta^{1-\kappa_1}(t_{n+1}-\vartheta)^{\alpha-1}d\vartheta. \end{aligned} \tag{137}$$

We can get the following numerical scheme

$$\begin{aligned}
S(t_{n+1}) &= \frac{1-\alpha}{\mathscr{A}\mathscr{B}(\alpha)} t_n^{1-\kappa_1}\mathscr{G}_1(t_n,S_n,I_n,V_n) \\
&+ \frac{\alpha(\Delta t)^\alpha}{\Gamma(\alpha+1)}\sum_{j=2}^{n} t_{j-2}^{1-\kappa_1}\mathscr{G}_1(t_{j-2},S_{j-2},I_{j-2},V_{j-2})\times \mathbf{W_1} \\
&+ \frac{\alpha(\Delta t)^\alpha}{\Gamma(\alpha+2)\mathscr{A}\mathscr{B}(\alpha)}\sum_{j=2}^{n}\left[t_{j-1}^{1-\kappa_1}\mathscr{G}_1(t_{j-1},S_{j-1},I_{j-1},V_{j-1}) - t_{j-2}^{1-\kappa_1}\mathscr{G}_1(t_{j-2},S_{j-2},I_{j-2},V_{j-2})\right]\times \mathbf{W_2} \\
&\sum_{j=2}^{n}\left[t_{j}^{1-\kappa_1}\mathscr{G}_1(t_{j},S_{j},I_{j},V_{j}) - 2t_{j-1}^{1-\kappa_1}\mathscr{G}_1(t_{j-1},S_{j-1},I_{j-1},V_{j-1}) - t_{j-2}^{1-\kappa_1}\mathscr{G}_1(t_{j-2},S_{j-2},I_{j-2},V_{j-2})\right]\times \mathbf{W_3},
\end{aligned} \tag{138}$$

$$\begin{aligned}
I(t_{n+1}) &= \frac{1-\alpha}{\mathscr{A}\mathscr{B}(\alpha)} t_n^{1-\kappa_1}\mathscr{G}_2(t_n,S_n,I_n,V_n) \\
&+ \frac{\alpha(\Delta t)^\alpha}{\Gamma(\alpha+1)}\sum_{j=2}^{n} t_{j-2}^{1-\kappa_1}\mathscr{G}_2(t_{j-2},S_{j-2},I_{j-2},V_{j-2})\times \mathbf{W_1} \\
&+ \frac{\alpha(\Delta t)^\alpha}{\Gamma(\alpha+2)\mathscr{A}\mathscr{B}(\alpha)}\sum_{j=2}^{n}\left[t_{j-1}^{1-\kappa_1}\mathscr{G}_2(t_{j-1},S_{j-1},I_{j-1},V_{j-1}) - t_{j-2}^{1-\kappa_1}\mathscr{G}_2(t_{j-2},S_{j-2},I_{j-2},V_{j-2})\right]\times \mathbf{W_2} \\
&\sum_{j=2}^{n}\left[t_{j}^{1-\kappa_1}\mathscr{G}_2(t_{j},S_{j},I_{j},V_{j}) - 2t_{j-1}^{1-\kappa_1}\mathscr{G}_2(t_{j-1},S_{j-1},I_{j-1},V_{j-1}) - t_{j-2}^{1-\kappa_1}\mathscr{G}_2(t_{j-2},S_{j-2},I_{j-2},V_{j-2})\right]\times \mathbf{W_3},
\end{aligned} \tag{139}$$

$$\begin{aligned}
V(t_{n+1}) &= \frac{1-\alpha}{\mathscr{A}\mathscr{B}(\alpha)} t_n^{1-\kappa_1}\mathscr{G}_3(t_n,S_n,I_n,V_n) \\
&+ \frac{\alpha(\Delta t)^\alpha}{\Gamma(\alpha+1)}\sum_{j=2}^{n} t_{j-2}^{1-\kappa_1}\mathscr{G}_3(t_{j-2},S_{j-2},I_{j-2},V_{j-2})\times \mathbf{W_1} \\
&+ \frac{\alpha(\Delta t)^\alpha}{\Gamma(\alpha+2)\mathscr{A}\mathscr{B}(\alpha)}\sum_{j=2}^{n}\left[t_{j-1}^{1-\kappa_1}\mathscr{G}_3(t_{j-1},S_{j-1},I_{j-1},V_{j-1}) - t_{j-2}^{1-\kappa_1}\mathscr{G}_3(t_{j-2},S_{j-2},I_{j-2},V_{j-2})\right]\times \mathbf{W_2} \\
&\sum_{j=2}^{n}\left[t_{j}^{1-\kappa_1}\mathscr{G}_3(t_{j},S_{j},I_{j},V_{j}) - 2t_{j-1}^{1-\kappa_1}\mathscr{G}_3(t_{j-1},S_{j-1},I_{j-1},V_{j-1}) - t_{j-2}^{1-\kappa_1}\mathscr{G}_3(t_{j-2},S_{j-2},I_{j-2},V_{j-2})\right]\times \mathbf{W_3}.
\end{aligned} \tag{140}$$

5.9 Numerical Simulations and Discussion

The non-linear epidemiological model of an infectious disease with vaccination has been studied mathematically. Numerous numerical simulations according to the parameter values are conducted to evaluate the role of the fractional derivative on the vaccination sections as a way to recognize the sound effects caused by the parameters employed in this infectious dynamics model. The model provides numerical representations for different fractional values that are consistent with the steady-state point using the fractal fractional derivative. Numerous numerical techniques can easily be employed to examine the end-time value of a certain parameter as a way to investigate how various factors affect the dynamics of the fractional order infectious model. Figures (15) through (17) display graphs of approximations of solutions against various fractional orders. As shown in figures (15)-(17) according to exponential decay kernel, power law kernel and Mittag Leffler kernel of the proposed system $S(t)$,I(t) and $R(t)$ rise as fractional values fall. The behaviour in all figures changes as the fractional values are decreased, indicating that the solution will be more successful if the fractional values are lower than the classical derivative. These simulations demonstrate how variations in value have an effect on the model's behaviour. Additionally, the simulation clearly illustrates how the condition of persons who have tuberculosis would change over time. As a result, the study becomes even more crucial for making choices and putting controls in place.

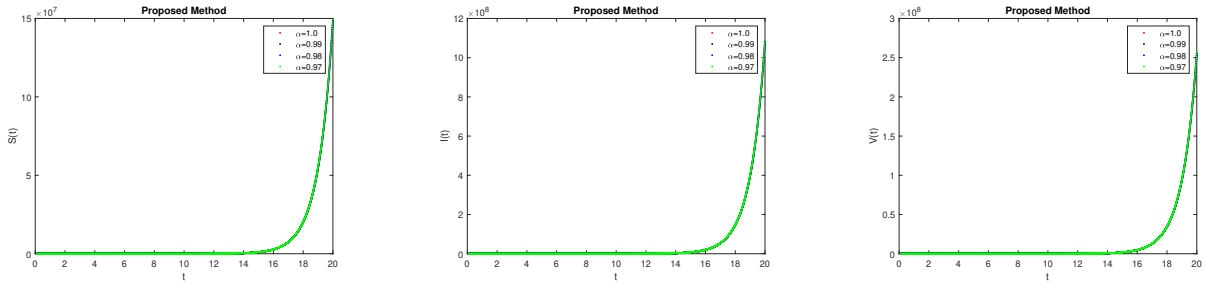

(a) $S(t)$ at $\alpha = 0.1, \kappa_1 = 0.01$ (b) $I(t)$ at $\alpha = 0.1, \kappa_1 = 0.01$ (c) $V(t)$ at $\alpha = 0.1, \kappa_1 = 0.01$

Fig. 15: Simulation of Compartments of Model with Exponential Decay kernel

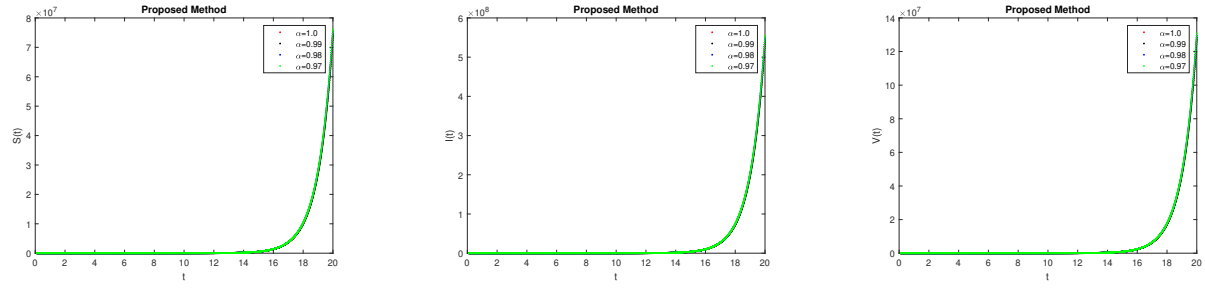

(a) $S(t)$ at $\alpha = 0.1, \kappa_1 = 0.01$ (b) $I(t)$ at $\alpha = 0.1, \kappa_1 = 0.01$ (c) $V(t)$ at $\alpha = 0.1, \kappa_1 = 0.01$

Fig. 16: Simulation of Compartments of Model with Power Law kernel

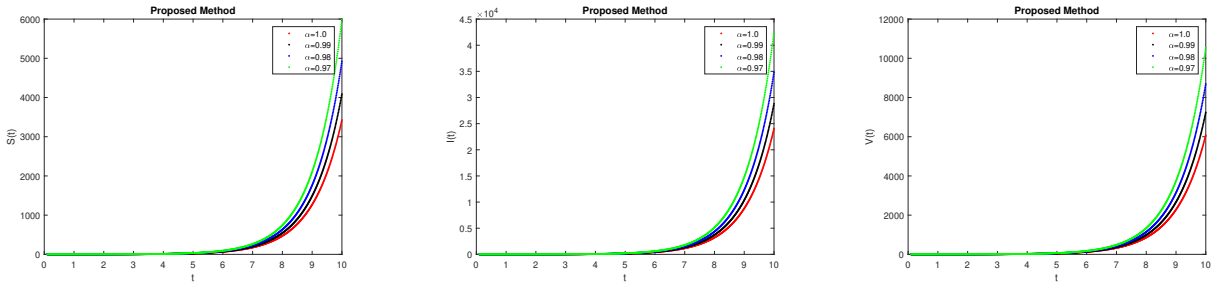

(a) $S(t)$ at $\alpha = 0.1, \kappa_1 = 0.01$ (b) $I(t)$ at $\alpha = 0.1, \kappa_1 = 0.01$ (c) $V(t)$ at $\alpha = 0.1, \kappa_1 = 0.01$

Fig. 17: Simulation of Compartments of Model with Mittag Leffler kernel

6 Conclusion

In the past two years, publishers, chief writers, and younger researchers have voiced concerns about the division that has developed within the field of fractional calculus. The splitting came about as a consequence of the creation of fractional differential operators with non-singular kernels, which in reality sparked a revolution in this area by providing fresh opportunities for both theoretical and practical uses of fractional calculus. However, certain scholars believed that differential operators with non-singular kernels and fractional derivatives with singular kernels would both satisfy the conditions of the classical derivative in a comparable manner for a variety of reasons. This defies logic since these

operators do quite different tasks. As a result, a fresh mathematical model was developed to show how fractional calculus will live on. If real data are used to run the numerical simulations, the behaviour of each class of the model under an erroneous increase in time may be assessed. This will show that the model is reliable. Mathematics in biology is one of the fields with the quickest development rates since it helps in the prediction of the emergence and resurgence of non-infectious diseases. These projections and forecasts can be made using integer and fractional-order modelling, which includes ordinary or partial differential equations. Fractional derivatives more specifically have shown a memory effect and hereditary qualities, giving them an additional trustworthy tool for forecasting the underlying dynamics of real-world systems in a number of fields of science and engineering. By defining derivatives and integrals for any real order, fractional calculus is a modification of traditional calculus. In systems with high-order movements and complicated nonlinear processes, fractional operators are more accurate at mimicking some occurrences than ordinary derivatives and ordinary integrals. There are two basic causes for this. Mathematical fractional techniques and research of excellent quality have improved our ability to anticipate and manage infectious diseases. Administrators in crisis can utilize the fractional order of the derivative, which can be employed for simulating not promotional infections at the microscopic level, to calculate the behaviour of infection. We suggested the Covid-19 model with a modified kernel for future direction utilizing fractional derivative. We may decide to do additional research on this topic later on as a result of the new information. For instance, the mathematical model can be changed by considering numerous dynamical patterns and looking at those structures using numerous derivatives.

This article provided fresh analysis that might be more useful for teaching, for example, about how infectious diseases propagate. This study investigated the stability of the reproduction number obtained by computing the reproduction number as the second derivative of the nonlinear component of an infectious class. The second derivative of the Lyapunov function and the sign of the second derivative of every category were employed in recognizing the waves. The mathematical model was subsequently solved using a numerical strategy based on Newton's polynomial interpolation. The deterministic infectious model's rate of reproduction and results showed that the fractional derivative field was long-lived. This is significant not only as a huge number of entrants will continue to enter this industry, but the reality that only a small part of its current uses are really in use. Consequently, despite the very few articles that have been published in opposition to them, the use of fractional differential and integral operators with nonsingular kernels will endure and be prevalent in all fields of science, technology, and engineering to arrive at useful conclusions. The past few years have seen a rise in the use of fractional derivatives in non-commercial models. The main advantage of fractional calculus is the possibility to simulate memory effects. In comparison to classical models, fractional models also provide a higher degree of freedom, making them very advantageous for fitting real data when it is provided. Additionally, fractional epidemic models that use multiple numerical methods to adapt mathematical models to real-world information can aid relevant organizations in avoiding or reducing the spread of infectious diseases in society. These findings are particularly beneficial to medical professionals in terms of planning, putting control methods into practice, the effects of treatment, and the spread of diseases to prevent infection in society and save lives.

Acknowledgment:
"This study was sponsored by the Prince Sattam bin Abdulaziz University via project number 2023/RV/04"

References

[1] A. Huppert and G. Katriel, Mathematical modelling and prediction in infectious disease epidemiology, *Clin. Microbiol. Infec.* **19**(11), 999-1005 (2013).
[2] A. L. P. da Costa, O. A. R. Neto and A. C. S. Silva-Júnior, Conditioners of the infectious diseases dynamics, *Estação Científica (UNIFAP)* **8**(3), 09-23 (2019).
[3] Z. Wang, M. A. Andrews, Z. X. Wu, L. Wang and C. T. Bauch, Coupled disease–behavior dynamics on complex networks: A review, *Phys. Life Rev.* **15**, 1-29 (2015).
[4] A. S. Fauci, Infectious diseases: considerations for the 21st century, *Clin. Infect. Dis.* **32**(5), 675-685 (2001).
[5] N. Puri, E. A. Coomes, H. Haghbayan and K. Gunaratne, Social media and vaccine hesitancy: new updates for the era of COVID-19 and globalized infectious diseases, *Human Vacc. Immunother.* **16**(11), 2586-2593 (2020).
[6] T. Wu, C. Perrings, A. Kinzig, J. P. Collins, B. A. Minteer and P. Daszak, Economic growth, urbanization, globalization, and the risks of emerging infectious diseases in China: a review, *Ambio.* **46**, 18-29 (2017).
[7] P. Roeder, J. Mariner and R. Kock, Rinderpest: the veterinary perspective on eradication, *Philosoph. Transac. Royal Soci. B: Biol. Sci.* **368**(1623), 20120139 (2013).
[8] R. Baker, A. Mahmud and I. E. Miller, Infectious disease in an era of global change, *Nat. Rev. Microbiol*, **20**, 193-205 (2022)(2021).
[9] H. W. Hethcote, The mathematics of infectious diseases, *SIAM Rev.* **42**(4), 599-653 (2000).
[10] H. Heesterbeek, R. M. Anderson, V. Andreasen, S. Bansal, D. De Angelis, C. Dye, et al., Isaac Newton Institute IDD collaboration, modeling infectious disease dynamics in the complex landscape of global health, *Sci.* **347**(6227), aaa4339 (2015).

[11] Z. Odibat and D. Baleanu, A new fractional derivative operator with generalized cardinal sine kernel: Numerical simulation *Math Comput Simul.*, **212**, 224-233 (2023).
[12] Z. Odibat and D. Baleanu, New Solutions of the Fractional Differential Equations With Modified Mittag-Leffler Kernel, *J. Comput. Nonlinear Dynam.* **18**(9), 091007 (2023).
[13] M. Rafei, M.I. Syam and D. Baleanu, Analytical Treatments to Systems of Fractional Differential Equations with Modified Atangana-Baleanu Derivative, *Fractal* S0218348X23401564 (2023).
[14] J.P. Singh, T. Abdeljawad, D. Baleanu and S. Kumar Transmission dynamics of a novel fractional model for the Marburg virus and recommended actions, *Eur. Phys. J.: Spec. Top.* **96**, 1-11 (2023).
[15] S. Javeed, Z.U. Abdeen, D. Baleanu, Fractional Modeling of Cancer with Mixed Therapies, *Front. Biosci. FRONT BIOSCI-LANDMRK* **28**(8), 174 (2023).
[16] A. Raza, D. Baleanu, T.N. Cheema, E. Fadhal, R.I.H. Ibrahim and N. Abdelli, Artificial intelligence computing analysis of fractional order COVID-19 epidemic model, *AIP Adv.* **13**(8),085017 (2023).
[17] K. Chatterjee, A. Kumar and S. Shankar, Healthcare impact of COVID-19 epidemic in India: A stochastic mathematical model, *Med. J. Armed For. India* **76**(2), 147-155 (2020).
[18] M. Kizito and J. Tumwiine, A mathematical model of treatment and vaccination interventions of pneumococcal pneumonia infection dynamics, *J. Appl. Math.*, (2018).
[19] B. Ivorra, M. R. Ferrández, M. Vela-Pérez and A. M. Ramos, Mathematical modeling of the spread of the coronavirus disease 2019 (COVID-19) taking into account the undetected infections. The case of China, *Commun. Nonlin. Sci. Numer. Sim.* **88**, 105303 (2020).
[20] A. J. Kucharski, T. W. Russell, C. Diamond, Y. Liu, J. Edmunds, S. Funk, S. Flasche, Early dynamics of transmission and control of COVID-19: a mathematical modelling study, *Lancet Infect. Dis.* **20**(5), 553-558 (2020).
[21] Z. Zhang, A. Zeb, O. F. Egbelowo and V. S. Erturk, Dynamics of a fractional order mathematical model for COVID-19 epidemic, *Adv. Differ. Equ.* **2020**(1), 1-16 (2020).
[22] S. Yadav, D. Kumar, J. Singh and D. Baleanu, Analysis and dynamics of fractional order Covid-19 model with memory effect, *Res. Phys.* **24**, 104017 (2021).
[23] M. Farman, A. Akgül, K. S. Nisar, D. Ahmad, A. Ahmad, S. Kamangar and C. A. Saleel, Epidemiological analysis of fractional order COVID-19 model with Mittag-Leffler kernel, *AIMS Math.* **7**(1), 756-783 (2022).
[24] M. ur Rahman, M. Arfan, K. Shah and J. F. Gómez-Aguilar, Investigating a nonlinear dynamical model of COVID-19 disease under fuzzy caputo, random and ABC fractional order derivative, *Chaos Solit. Fract.* **140**, 110232 (2020).
[25] A. Khan, J. F. Gómez-Aguilar, T. S. Khan and H. Khan, Stability analysis and numerical solutions of fractional order HIV/AIDS model, *Chaos Solit. Fract.* **122**, 119-128 (2019).
[26] A. Babaei, H. Jafari and M. Ahmadi, A fractional order HIV/AIDS model based on the effect of screening of unaware infectives, *Math. Meth. Appl. Sci.* **42**(7), 2334-2343 (2019).
[27] M. Farman, A. Akgül, M. T. Tekin, M. M. Akram, A. Ahmad, E. E. Mahmoud and I. S. Yahia, Fractal fractional-order derivative for HIV/AIDS model with Mittag-Leffler kernel, *Alexandria Eng. J.* **61**(12), 10965-10980 (2022).
[28] W.H. Huang, M. Samraiz, A. Mehmood, D. Baleanu, G. Rahman and S. Naheed, Modified Atangana-Baleanu fractional operators involving generalized Mittag-Leffler function, *Alexandria Eng. J.* **75** 639-648 (2022).
[29] M. Rahman, M. Arfan and D. Baleanu, Piecewise fractional analysis of the migration effect in plant-pathogen-herbivore interactions, *Bull. Math. Biol.* **1**(1), 1-23 (2023).
[30] Z. Alijani, B. Shiri, I. Perfilieva and D Baleanu, Numerical solution of a new mathematical model for intravenous drug administration, *Evol. Intell.* 1-17 (2023).
[31] F. Bozkurt, A. Yousef, H. Bilgil and D. Baleanu A mathematical model with piecewise constant arguments of colorectal cancer with chemo-immunotherapy, *Chaos Solit. Fractals* **168**,113207 (2023).
[32] K. Umapathy, B. Palanivelu, R. Jayaraj, D. Baleanu and P.B. Dhandapani, On the decomposition and analysis of novel simultaneous SEIQR epidemic model, *AIMS math.* **8**(3), 5918-5933 (2023).
[33] World Health Organization. Ebola virus disease. Fact sheet N 103. Updated September 2014.
[34] T. Berge, J. S. Lubuma, G. M. Moremedi, N. Morris and R. Kondera-Shava, A simple mathematical model for Ebola in Africa, *J. Biol. Dyn.* **11**(1), 42-74 (2017).
[35] G. Chowell and H. Nishiura, Transmission dynamics and control of Ebola virus disease (EVD): a review, *BMC Med.* **12**, 1-17 (2014).
[36] S. T. Jacob, I. Crozier, W. A. Fischer, A. Hewlett, C. S. Kraft, M. A. D. L. Vega and J. H. Kuhn, Ebola virus disease, *Nature Rev. Dis. Prim.* **6**(1), 13 (2020).
[37] F. Ndaïrou, M. Khalighi and L. Lahti, Ebola epidemic model with dynamic population and memory, *Chaos Solit. Fract.* **170**, 113361 (2023).
[38] F. B. Agusto, Mathematical model of Ebola transmission dynamics with relapse and reinfection, *Math. Biosci.* **283**, 48-59 (2017).
[39] A. Rachah, A mathematical model with isolation for the dynamics of Ebola virus. In Journal of Physics: Conference Series (Vol. 1132, No. 1, p. 012058). IOP Publishing, (2018, November).
[40] M. Farman, A. Akgül, T. Abdeljawad, P. A. Naik, N. Bukhari and A. Ahmad, Modeling and analysis of fractional order Ebola virus model with Mittag-Leffler kernel, *Alexandria Eng. J.* **61**(3), 2062-2073 (2022).
[41] P. Anand, A. B. Kunnumakara, C. Sundaram, K. B. Harikumar, S. T. Tharakan, O. S. Lai, and B. B. Aggarwal, Cancer is a preventable disease that requires major lifestyle changes, *Pharmac. Res.* **25**, 2097-2116 (2008).

[42] S. F. Moss and M. J. Blaser, Mechanisms of disease: inflammation and the origins of cancer, *Nature Clin. Prac. Oncol.* **2**(2), 90-97 (2005).
[43] World Health Organization, Strategy for cancer prevention and control in the Eastern Mediterranean Region 2009-2013 (No. WHO-EM/NCD/064/E), 2010.
[44] A. A. Wani, Cancer: its symptoms, challenges and opportunities in research in India: a review, *Saudi J. Med. Pharm. Sci.* **9**(1), 1-5 (2023).
[45] P. M. Altrock, L. L. Liu and F. Michor, The mathematics of cancer: integrating quantitative models, *Nature Rev. Can.* **15**(12), 730-745 (2015).
[46] S. K. Panda, A. Atangana and T. Abdeljawad, Existence results and numerical study on novel Coronavirus 2019-Ncov/Sars-Cov-2 model using differential operators based on the generalized Mittag-Leffler kernel and fixed points, *Fract.* **30**(08), 2240214 (2022).
[47] A. Atangana and E. F. D. Goufo, Modern and generalized analysis of exogenous growth models, *Chaos Solit. Fract.* **163**, 112605 (2022).
[48] A. Atangana and S. Igret Araz, Advanced analysis in epidemiological modeling: Detection of wave, *medRxiv*, 2021-09 (2021).
[49] A. Atangana and I. Koca, Chaos in a simple nonlinear system with Atangana–Baleanu derivatives with fractional order, *Chaos Solit. Fract.* **89**, 447-454 (2016).
[50] A. Atangana and D. Baleanu, New fractional derivatives with nonlocal and non-singular kernel: theory and application to heat transfer model, **20**(2), 763-769 (2016).
[51] A. Atangana, On the new fractional derivative and application to nonlinear Fisher's reaction–diffusion equation, *Appl. Math. Comput.* **273**, 948-956 (2016).
[52] A. Atangana and B. S. T. Alkahtani, Analysis of the Keller–Segel model with a fractional derivative without singular kernel, *Entropy* **17**(6), 4439-4453 (2015).
[53] A. Atangana and A. Secer, A note on fractional order derivatives and table of fractional derivatives of some special functions, *Abstr. Appl. Anal.* **2013**, (2013).
[54] Z. Tchoundjeu, E. K. Asaah, P. Anegbeh, A. Degrande, P. Mbile, C. Facheux and A. J. Simons, Putting participatory domestication into practice in West and Central Africa, *Forest. Tre. Livel.* **16**(1), 53-69 (2006).
[55] R. T. Kamga, C. Kouamé, A. R. Atangana, T. Chagomoka, and R. Ndango, Nutritional evaluation of five African indigenous vegetables, *J. Horticult. Res.* **21**(1), 99-106 (2013).
[56] J. F. Gómez-Aguilar and A. Atangana, New insight in fractional differentiation: power, exponential decay and Mittag-Leffler laws and applications, *Eur. Phys. J. Plus* **132**, 1-21 (2017).
[57] D. Baleanu, A. Jajarmi, H. Mohammadi and S. Rezapour, A new study on the mathematical modelling of human liver with Caputo–Fabrizio fractional derivativ, *Chaos Solit. Fract.* **134**, 109705 (2020).
[58] A. Jajarmi, D. Baleanu, S. S. Sajjadi and J. J. Nieto, Analysis and some applications of a regularized ψ-Hilfer fractional derivative, *J. Comput. Appl. Math.* **415**, 114476 (2022).
[59] K. Shah, M. Sinan, T. Abdeljawad, M. A. El-Shorbagy, B. Abdalla and M. S. Abualrub, A detailed study of a fractal-fractional transmission dynamical model of viral infectious disease with vaccination, *Complexity* **2022**, (2022).
[60] A. Malik, N. Kumar and K. Alam, Estimation of parameter of fractional order COVID-19 SIQR epidemic model, *Mater. Today Proc.* **49**, 3265-3269 (2022).
[61] C. N. Angstmann, B. I. Henry and A. V. McGann, A fractional-order infectivity and recovery SIR model, *Fract. Fract.* **1**(1), 11 (2017).
[62] S. Pooseh, H. S. Rodrigues and D. F. Torres, Fractional derivatives in dengue epidemics, In AIP Conference Proceedings (Vol. 1389, No. 1, pp. 739-742). American Institute of Physics, 2011
[63] K. Diethelm, A fractional calculus based model for the simulation of an outbreak of dengue fever, *Nonlin. Dyn.* **71**, 613-619 (2013).
[64] O. S. Iyiola and F. D. Zaman, A fractional diffusion equation model for cancer tumor, *AIP Adv.* **4**(10), 107121 (2014).
[65] A. Ullah, T. Abdeljawad, S. Ahmad and K. Shah, Study of a fractional-order epidemic model of childhood diseases, *J. Func. Space.* **2020**, (2020).
[66] M. Mandal, S. Jana, S. K. Nandiand T. K. Kar, Modelling and control of a fractional-order epidemic model with fear effect, *Energ. Ecol. Envir.* **5**(6), 421-432 (2020).
[67] G. González-Parra, A. J. Arenas and B. M. Chen-Charpentier, A fractional order epidemic model for the simulation of outbreaks of influenza A (H1N1), *Math. Meth. Appl. Sci.* **37**(15), 2218-2226 (2014).
[68] S. He and S. Banerjee, Epidemic outbreaks and its control using a fractional order model with seasonality and stochastic infection, *Physica A: Stat. Mech. App.* **501**, 408-417 (2018).
[69] A. Atangana and S. Rashid, Analysis of a deterministic-stochastic oncolytic M1 model involving immune response via crossover behaviour: ergodic stationary distribution and extinction, *AIMS Math.* **8**(2), 3236-3268 (2023).
[70] A. Atangana and I. Koca, Analytical and numerical investigation of the Hindmarsh-Rose model neuronal activity, *Math. Biosci. Engin.* **20**(1), 1434-1459 (2023).
[71] C. N. Angstmann, B. I. Henry and A. V. McGann, A fractional order recovery SIR model from a stochastic process, *Bull. Math. Biol.* **78**, 468-499 (2016).
[72] M. R. Sidi Ammi, M. Tahiri, M. Tilioua, A. Zeb, I. Khan and M. Andualem, Global analysis of a time fractional order spatio-temporal SIR model, *Sci. Rep.* **12**(1), 5751 (2022).

[73] T. Li, Y. Wang, F. Liu and I. Turner, Novel parameter estimation techniques for a multi-term fractional dynamical epidemic model of dengue fever, *Numer. Algr.* **82**, 1467-1495 (2019).
[74] K. Windarto and F. Khan, Parameter estimation and fractional derivatives of dengue transmission model, *AIMS Math.* **5**(3), 2758-2779 (2020).
[75] N. P. Dong, H. V. Long and A. Khastan, Optimal control of a fractional order model for granular SEIR epidemic with uncertainty, *Commun. Nonlin. Sci. Numer. Sim.* **88**, 105312 (2020).
[76] S. Ahmad, A. Ullah, K. Shah, S. Salahshour, A. Ahmadian and T. Ciano, Fuzzy fractional-order model of the novel coronavirus, *Adv. Differ. Equ.* **2020**(1), 1-17 (2020).
[77] A. S. Shaikh, I. N. Shaikh and K. S. Nisar, A mathematical model of COVID-19 using fractional derivative: outbreak in India with dynamics of transmission and control, *Adv. Differ. Equ.* **2020**(1), 1-19.
[78] V. Lakshmikantham, S. Leela and J. V. Devi, Theory of fractional dynamic systems, 2009.
[79] Y. A. Rossikhin and M. V. Shitikova, Applications of fractional calculus to dynamic problems of linear and nonlinear hereditary mechanics of solids, *50*(1), 15-67 (1997).
[80] F. Haq, K. Shah, G.U. Rahman and M. Shahzad, Numerical analysis of fractional order model of HIV-1 infection of CD4+ T-cells, *Comput. Meth. Diff. Equ.* **5**(1), 1-11 (2017).
[81] A. Khan, T. S. Khan, M. I. Syam and H. Khan, Analytical solutions of time-fractional wave equation by double Laplace transform method, *Eur. Phys. J. Plus* **134**(4), 163 (2019).
[82] B. Acay, E. Bas and T. Abdeljawad, Fractional economic models based on market equilibrium in the frame of different type kernels, *Chaos Soliton. Fract.* **130**, 109438 (2020).
[83] M. Farman, A. Akgül, H. Shanak, J. Asad and A. Ahmad, Computer Virus Fractional Order Model with Effects of Internal and External Storage Media, *Eur. J. Pure Appl. Math.* **15**(3), 897-915 (2022).
[84] M. M. Ghalib, A. A. Zafar, M. Farman, A. Akgül, M. O. Ahmad and A. Ahmad, Unsteady MHD flow of Maxwell fluid with Caputo–Fabrizio non-integer derivative model having slip/non-slip fluid flow and Newtonian heating at the boundary, *Ind. J. Phy.* **96**(1), 127-136 (2022).
[85] N. Gul, R. Bilal, E. A. Algehyne, M. G. Alshehri, M. A. Khan, Y. M. Chu and S. Islam, The dynamics of fractional order Hepatitis B virus model with asymptomatic carriers, *Alexandria Eng. J.* **60**(4), 3945-3955 (2021).
[86] A. Jajarmi and D. Baleanu, A new fractional analysis on the interaction of HIV with CD4+ T-cells, *Chaos Solit. Fract.* **113**, 221-229 (2018).
[87] I. Ullah, S. Ahmad, M. ur Rahman and M. Arfan, Investigation of fractional order tuberculosis (TB) model via Caputo derivative, *Chaos Solit. Fract.* **142**, 110479 (2021).
[88] T. Khan, R. Ullah, G. Zaman and J. Alzabut, A mathematical model for the dynamics of SARS-CoV-2 virus using the Caputo-Fabrizio operator, *Math. Biosci. Eng.* **18**(5), 6095-6116 (2021).
[89] P. Liu, T. Munir, T. Cui, and P. Wu, Mathematical assessment of the dynamics of the tobacco smoking model: An application of fractional theory, *AIMS Math.* **7**(4), 7143-7165 (2022).
[90] A. Atangana, E. Bonyah and A. A. Elsadany, A fractional order optimal 4D chaotic financial model with Mittag-Leffler law, *Chin. J. Phys.* **65**, 38-53 (2020).
[91] M. Al-Refai and D. Baleanu, On an extension of the operator with Mittag-Leffler kernel, *Fractals* **30**(05), 1-7 (2022).
[92] R. Kanno, Representation of random walk in fractal space-time, *Physica A: Stat. Mech. App.* **248**(1-2), 165-175 (1998).
[93] D. R. Anderson and D. J. Ulness, Newly defined conformable derivatives, *Adv. Dyn. Syst. Appl.* **10**(2), 109-137 (2015).
[94] D. Baleanu, A. Fernandez and A. Akgül, On a fractional operator combining proportional and classical differintegrals, *Math.* **8**(3), 360 (2020).
[95] I. Ahmed, P. Kumam, F. Jarad, P. Borisut and W. Jirakitpuwapat, On Hilfer generalized proportional fractional derivative, *Adv. Differ. Equ.* **2020**(1), 1-18 (2020).
[96] R. E. Baker, A. S. Mahmud, I. F. Miller, M. Rajeev, F. Rasambainarivo, B. L. Riceand C. J. E. Metcalf, Infectious disease in an era of global change, *Nature Rev. Micr.* **20**(4), 193-205 (2022).
[97] W. M. Sweileh, Global research activity on mathematical modeling of transmission and control of 23 selected infectious disease outbreak, *Globaliz. Health* **18**(1), 1-14 (2022).
[98] A. A. Thirthar, H. Abboubakar, A. Khan and T. Abdeljawad, Mathematical modeling of the COVID-19 epidemic with fear impact, *AIMS Math.* **8**(3), 6447-6465 (2023).
[99] Q. Zhang, X. Liu, Q. Li, Y. Liu, H. He, K. Wang and Z. Yan, Quantitative model for assessment of lower-extremity perfusion in patients with diabetes, *Med. Phys.*, (2023).
[100] J. Andrawus, S. Abdulrahman, R. V. K. Singh and S. S. Manga, Optimal control of mathematical modelling for Ebola virus population dynamics in the presence of vaccination, *Dutse J. Pure Appl. Sci.* **8**, 126-137 (2022).
[101] A. Ahmad, M. Farman, A. Ghafar, M. Inc, M. O. Ahmad and N. Sene, Analysis and simulation of fractional order smoking epidemic model, *Comput. Math. Meth. Med.* **2022**, (2022).
[102] M. Farman, A. Shehzad, A. Akgül, D. Baleanu, M. D. L. Sen, Modelling and analysis of a measles epidemic model with the constant proportional Caputo operator, *Symmetry* **15**(2), 468 (2023).
[103] P.Dhanalakshmi, S. Senpagam and R. Mohanapriya, Finite-time fuzzy reliable controller design for fractional-order tumor system under chemotherapy, *Fuzzy Set. Sys.* **432**, 168-181 (2022).
[104] M. Abaid Ur Rehman, J. Ahmad, A. Hassan, J. Awrejcewicz, W. Pawlowski, H. Karamti and F. M. Alharbi, The Dynamics of a Fractional-Order Mathematical Model of Cancer Tumor Disease, *Symmetry* **14**(8), 1694 (2022).

[105] M. Helikumi and P. O. Lolika, Global Dynamics of Fractional-order Model for Malaria Disease Transmission, *Asian Res. J. Math.*, **18**(9), 82-110 (2022).
[106] X. Cui, D. Xue and T. Li, Fractional-order delayed Ross–Macdonald model for malaria transmission, *Nonlin. Dyn.* **107**(3), 3155-3173 (2022).
[107] M. S. Arif, A. Raza, M. Rafiq, M. Bibi, R. Fayyaz, M. Naz and U. Javed, A reliable stochastic numerical analysis for typhoid fever incorporating with protection against infection, *Comput. Mater. Cont.* **59**(3), 787-804 (2019).
[108] M. Sinan, K. Shah, P. Kumam, I. Mahariq, K. J. Ansari, Z. Ahmad and Z. Shah, Fractional order mathematical modeling of typhoid fever disease, *Result. Phys.* **32**, 105044 (2022).
[109] F. M. Khan, Z. U. Khan, Y. P. Lv, A. Yusuf and A. Din, Investigating of fractional order dengue epidemic model with ABC operator, *Result. Phys.* **24**, 104075 (2021).
[110] B. Karaagac, K. M. Owolabi and K. S. Nisar, Analysis and dynamics of illicit drug use described by fractional derivative with Mittag-Leffler kernel, *CMC-Comput. Mater. Cont.* **65**(3), 1905-1924 (2020).
[111] M. Rafiq, A. Raza, M. U. Iqbal, Z. Butt, H. A. Naseem, M. A. Akram and S. Azam, Numerical treatment of stochastic heroin epidemic model, *Adv. Differ. Equ.* **2019**, 1-17 (2019).
[112] S. Rashid, F. Jarad, A. G. Ahmad and K. M. Abualnaja, New numerical dynamics of the heroin epidemic model using a fractional derivative with Mittag-Leffler kernel and consequences for control mechanisms, *Res. Phys.* **35**, 105304 (2022).
[113] Z. U. A. Zafar, H. Rezazadeh, M. Inc, K. S. Nisar, T. A. Sulaiman and A. Yusuf, Fractional order heroin epidemic dynamics, *Alexandria Engin. J.* **60**(6), 5157-5165 (2021).
[114] X. Wang, J. Yang and X. Li, Dynamics of a heroin epidemic model with very population, *Appl. Math.* **2**(6), 732 (2011).
[115] X. Li, R. P. Agarwal, J. F. Gomez-Aguilar, Q. Badshah and G. ur Rahman, Threshold dynamics: formulation, stability & sensitivity analysis of co-abuse model of heroin and smoking, *Chaos Solit. Fract.* **161**, 112373 (2022).
[116] S. A. Khan, K. Shah, G. Zaman and F. Jarad, Existence theory and numerical solutions to smoking model under Caputo-Fabrizio fractional derivative, *Chaos* **29**(1), 013128 (2019).
[117] E. Addai, L. Zhang, J. K. Asamoah and J. F. Essel, A fractional order age-specific smoke epidemic model, *Appl. Math. Model.* **119**, 99-118 (2023).
[118] Y. N. Anjam, R. Shafqat, I. E. Sarris, M. Ur Rahman, S. Touseef and M. Arshad, A fractional order investigation of smoking model using Caputo-Fabrizio differential operator, *Fract. Fract.* **6**(11), 623 (2022).
[119] A. Zeb, M. I. Chohan and G. Zaman, The homotopy analysis method for approximating of giving up smoking model in fractional order, (2012).
[120] Z. Alkhudhari, S. Al-Sheikh and S. Al-Tuwairqi, Global dynamics of a mathematical model on smoking, *International Scholarly Research Notices*, 2014.
[121] M. Khalid, F. S. Khan and A. Iqbal, Perturbation-iteration algorithm to solve fractional giving up smoking mathematical model, *Int. J. Comput. App.* **142**(9), 1-6 (2016).
[122] M. U. Saleem, M. Farman, A. Ahmad, E. U. Haque and M. O. Ahmad, A Caputo Fabrizio fractional order model for control of glucose in insulin therapies for diabetes, *Ain Shams Eng. J.* **11**(4), 1309-1316 (2020).
[123] A. Omame, U. K. Nwajeri, M. Abbas and C. P. Onyenegecha, A fractional order control model for Diabetes and COVID-19 co-dynamics with Mittag-Leffler function, *Alexandria Eng. J.* **61**(10), 7619-7635 (2022).
[124] S. Mollah, S. Biswas and S. Khajanchi, Impact of awareness program on diabetes mellitus described by fractional-order model solving by homotopy analysis method, *Ricerche di Matematica*, 1-26 (2022).
[125] G. Narayanan, M. S. Ali, G. Rajchakit, A. Jirawattanapanit and B. Priya, Stability analysis for Nabla discrete fractional-order of Glucose–Insulin Regulatory System on diabetes mellitus with Mittag-Leffler kernel, *Biomed. Signal Process. Cont.* **80**, 104295 (2023).
[126] A. Akgül, M. Farman, A. Ahmad, A. Khan, S. Zahran and W. S. Awad, Fractional Order Glucose Insulin Model with Generalized Mittag-Leffler Kernel, *Appl. Math.* **17**(2), 365-374 (2023).
[127] C. Z. Aguilar, J. F. Gómez-Aguilar, V. M. Alvarado-Martínez and H. M. Romero-Ugalde, Fractional order neural networks for system identification, *Chaos Solit. Fract.* **130**, 109444 (2020).
[128] E. Kaslik and S. Sivasundaram, Nonlinear dynamics and chaos in fractional-order neural networks, *Neural Netw.* **32**, 245-256 (2012).
[129] C. Xu, M. Liao, P. Li, Y. Guo, Q. Xiao and S. Yuan, Influence of multiple time delays on bifurcation of fractional-order neural networks, *Appl. Math. Comput.* **361**, 565-582 (2019).
[130] C. Xu, W. Zhang, Z. Liu and L. Yao, Delay-induced periodic oscillation for fractional-order neural networks with mixed delays, *Neurocomputing* **488**, 681-693 (2022).
[131] E. Tlelo-Cuautle, A. M. González-Zapata, J. D. Díaz-Muñoz, L. G. de la Fraga and I. Cruz-Vega, Optimization of fractional-order chaotic cellular neural networks by metaheuristics, *Eur. Phys. J. Spec. Topic.* **231**(10), 2037-2043 (2022).
[132] A. Ali, S. Islam, M. R. Khan, S. Rasheed, F. M. Allehiany, J. Baili and H. Ahmad, Dynamics of a fractional order Zika virus model with mutant, *Alexandria Engn. J.* **61**(6), 4821-4836 (2022).
[133] R. Begum, O. Tunç, H. Khan, H. Gulzar and A. Khan, A fractional order Zika virus model with Mittag–Leffler kernel, *Chaos Solit. Fract.* **146**, 110898 (2021).
[134] H. M. Ali and I. G. Ameen, Optimal control strategies of a fractional order model for Zika virus infection involving various transmissions, *Chaos Solit. Fract.* **146**, 110864 (2021).

[135] R. Rakkiyappan, V. P. Latha and F. A. Rihan, A fractional-order model for Zika virus infection with multiple delays, *Complexity* **2019**, 1-20 (2019).
[136] R. Prasad, K. Kumar and R. Dohare, Caputo fractional order derivative model of Zika virus transmission dynamics, *J. Math. Comput. Sci.* **28**(2), 145 (2023).
[137] T. B. Gashirai, S. D. Hove-Musekwa and S. Mushayabasa, Optimal control applied to a fractional-order foot-and-mouth disease model, *Int. J. Appl. Comput. Math.* **7**(3), 73 (2021).
[138] T. B. Gashirai, S. D. Hove-Musekwa and S. Mushayabasa, Dynamical analysis of a fractional-order foot-and-mouth disease model, *Math. Sci.* **15**(1), 65-82 (2021).
[139] R. Shi and T. Lu, Dynamic analysis and optimal control of a fractional order model for hand-foot-mouth disease, *J. Appl. Math. Comput.* **64**(1-2), 565-590 (2020).
[140] B. Ghanbari, A fractional system of delay differential equation with nonsingular kernels in modeling hand-foot-mouth disease, *Adv. Differ. Equ.* **2020**(1), 1-20 (2020).
[141] T. B. Gashirai, S. D. Hove-Musekwa and S. Mushayabasa, Lyapunov Stability Analysis of a Delayed Foot-and-Mouth Disease Model with Animal Vaccination, *Disc. Dyn. Nat. Soc.* **2020**, 1-13 (2020).
[142] R. Seck, D. Ngom, B. Ivorra and A. M. Ramos, An optimal control model to design strategies for reducing the spread of the Ebola virus disease, *Math. Biosci. Engin.* **19**(2), 1746-1774 (2022).
[143] A. Hasan, A. Akgül, M. Farman, F. Chaudhry, M. Sultan and M. De la Sen, Epidemiological analysis of symmetry in transmission of the Ebola virus with power law kernel, *Symmetry* **15**(3), 665 (2023).
[144] A. Muniyappan, B. Sundarappan, P. Manoharan, M. Hamdi, K. Raahemifar, S. Bourouis and V. Varadarajan, Stability and numerical solutions of second wave mathematical modeling on covid-19 and omicron outbreak strategy of pandemic: Analytical and error analysis of approximate series solutions by using hpm, *Math.* **10**(3), 343 (2022).
[145] M. Farman, H. Besbes, K. S. Nisar and M. Omri, Analysis and dynamical transmission of Covid-19 model by using Caputo-Fabrizio derivative, *Alexandria Eng. J.* **66**, 597-606 (2023).
[146] Z. U. A. Zafar, K. Rehan and M. Mushtaq, Retracted article: fractional-order scheme for bovine babesiosis disease and tick populations, *Adv. Differ. Equ.* **2017**(1), 1-19 (2017).
[147] A. Ahmad, M. Farman, P. A. Naik, N. Zafar, A. Akgul and M. U. Saleem, Modeling and numerical investigation of fractional-order bovine babesiosis disease, *Numer. Meth. Part. Diff. Equ.* **37**(3), 1946-1964 (2021).
[148] Jaharuddin and T. Bakhtiar, Control policy mix in measles transmission dynamics using vaccination, therapy, and treatment, *Int. J. Math. Math. Sci.* **2020**, 1-20 (2020).
[149] M. Parsamanesh, M. Erfanian and S. Mehrshad, Stability and bifurcations in a discrete-time epidemic model with vaccination and vital dynamics, *BMC Bioin.* **21**, 1-15 (2020).